Since January 2020 Elsevier has created a COVID-19 resource centre with free information in English and Mandarin on the novel coronavirus COVID-19. The COVID-19 resource centre is hosted on Elsevier Connect, the company's public news and information website.

Cell Reports

Article

Robust innate responses to SARS-CoV-2 in children resolve faster than in adults without compromising adaptive immunity

Graphical abstract

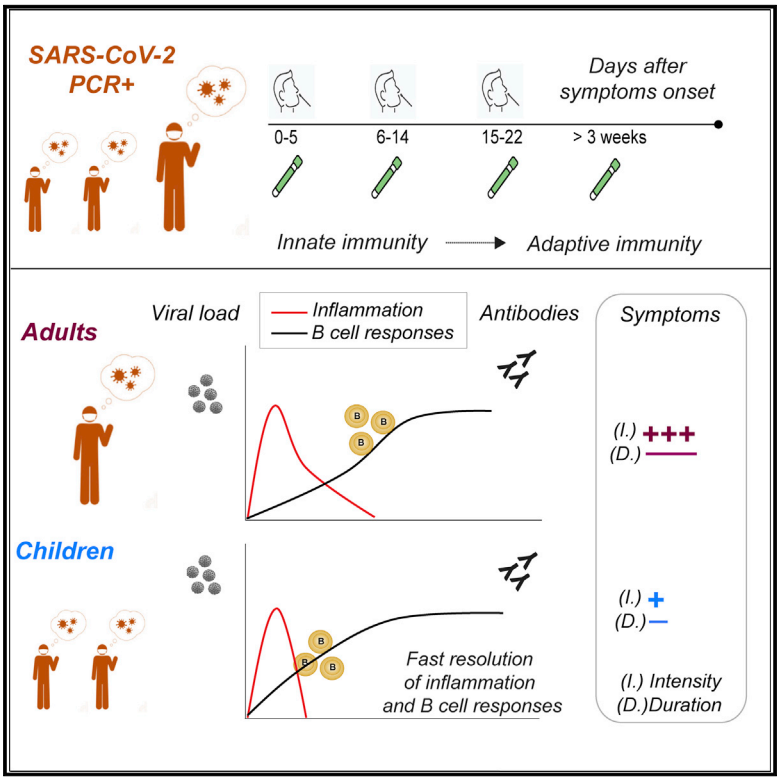

Highlights

- Innate response against SARS-CoV-2 is robust in children despite limited symptoms
- Resolution of inflammation and onset of B cell response occur faster in children
- Antibody response is not compromised by the shorter antiviral inflammatory response

Authors

Maria Vono, Angela Huttner, Sylvain Lemeille, ..., Geraldine Blanchard-Rohner, Claire-Anne Siegrist, Arnaud M. Didierlaurent

Correspondence

arnaud.didierlaurent@unige.ch

In brief

SARS-CoV-2 infection in children is less severe than it is in adults. Vono et al. find that children mount a potent, but more transient, antiviral innate response with a more rapid onset of B cell response. A more efficient early control of inflammation may be key to limiting disease severity.

Vono et al., 2021, Cell Reports *37*, 109773
October 5, 2021
https://doi.org/10.1016/j.celrep.2021.109773

CellPress

Cell Reports

CellPress
OPEN ACCESS

Article

Robust innate responses to SARS-CoV-2 in children resolve faster than in adults without compromising adaptive immunity

Maria Vono,[1,14] Angela Huttner,[1,2,3,4,14] Sylvain Lemeille,[1] Paola Martinez-Murillo,[1] Benjamin Meyer,[1] Stephanie Baggio,[5,6] Shilpee Sharma,[7] Anais Thiriard,[7] Arnaud Marchant,[7] Gert-Jan Godeke,[8] Chantal Reusken,[8] Catia Alvarez,[9] Francisco Perez-Rodriguez,[2,3] Isabella Eckerle,[3,9,10,11] Laurent Kaiser,[3,9,10,11] Natasha Loevy,[12] Christiane S. Eberhardt,[1] Geraldine Blanchard-Rohner,[1,13] Claire-Anne Siegrist,[1,2,15] and Arnaud M. Didierlaurent[1,11,15,16,*]

[1]Center of Vaccinology, Department of Pathology and Immunology, Faculty of Medicine, University of Geneva, Geneva, Switzerland
[2]University of Geneva Medical School, Geneva, Switzerland
[3]Division of Infectious Diseases, Geneva University Hospitals, Geneva, Switzerland
[4]Center for Clinical Research, Geneva University Hospitals and Faculty of Medicine, University of Geneva, Geneva, Switzerland
[5]Division of Prison Health, Geneva University Hospitals, Geneva, Switzerland
[6]Office of Corrections, Department of Justice and Home Affairs of the Canton of Zurich, Zurich, Switzerland
[7]Institute for Medical Immunology, Université libre de Bruxelles, Charleroi, Belgium
[8]Centre for Infectious Disease Control, National Institute for Public Health and the Environment (RIVM), Bilthoven, the Netherlands
[9]Department of Microbiology and Molecular Medicine, Faculty of Medicine, University of Geneva, 1205 Geneva, Switzerland
[10]Laboratory of Virology, Division of Laboratory Medicine, Geneva University Hospitals, Geneva, Switzerland
[11]Geneva Centre for Emerging Viral Diseases, Geneva University Hospitals, Geneva, Switzerland
[12]Pediatric Platform for Clinical Research, Department of Woman, Child and Adolescent Medicine, Geneva University Hospitals and Faculty of Medicine, University of Geneva, Geneva, Switzerland
[13]Unit of Immunology and Vaccinology, Division of General Pediatrics, Department of Pediatrics, Gynecology and Obstetrics, Geneva University Hospitals, University of Geneva, Geneva, Switzerland
[14]These authors contributed equally
[15]These authors contributed equally
[16]Lead contact
*Correspondence: arnaud.didierlaurent@unige.ch
https://doi.org/10.1016/j.celrep.2021.109773

SUMMARY

SARS-CoV-2 infection in children is less severe than it is in adults. We perform a longitudinal analysis of the early innate responses in children and adults with mild infection within household clusters. Children display fewer symptoms than adults do, despite similar initial viral load, and mount a robust anti-viral immune signature typical of the SARS-CoV-2 infection and characterized by early interferon gene responses; increases in cytokines, such as CXCL10 and GM-CSF; and changes in blood cell numbers. When compared with adults, the antiviral response resolves faster (within a week of symptoms), monocytes and dendritic cells are more transiently activated, and genes associated with B cell activation appear earlier in children. Nonetheless, these differences do not have major effects on the quality of SARS-CoV-2-specific antibody responses. Our findings reveal that better early control of inflammation as observed in children may be key for rapidly controlling infection and limiting the disease course.

INTRODUCTION

Clinical symptoms of SARS-CoV-2 infection are highly variable among individuals; it is not yet clear what determines that variability. A consistent finding is the effect of age on disease severity. The need for hospitalization for severe disease is relatively rare in children and adolescents (Castagnoli et al., 2020; Viner et al., 2021). Most children infected with SARS-CoV-2 remain asymptomatic or have mild symptoms, such as fever, cough, or gastrointestinal symptoms (Lu et al., 2020; Munro and Faust, 2020; Zimmermann and Curtis, 2020). The rare, but serious, condition known as multisystem inflammatory syndrome in children (MIS-C) after SARS-CoV-2 exposure has features that differ from those of severe COVID-19 (Consiglio et al., 2020; Grazioli et al., 2021; Riphagen et al., 2020; Verdoni et al., 2020). Although it is critical to understand why some children develop severe COVID-19 or MIS-C, it is equally important to understand the basis for the relative resistance of children to symptomatic infection.

The pattern of SARS-CoV-2 infection in children contrasts with that of other respiratory infections, such as respiratory syncytial virus (RSV) or influenza, which inflicts a greater burden of

hospitalization and severe disease on young children compared with that of adolescents (Matias et al., 2016; Shi et al., 2017). Reasons for this apparent reduced susceptibility to severe SARS-CoV-2 infection remain unclear, but several hypotheses have been proposed (Brodin, 2020; Midulla et al., 2020; Wong et al., 2020). The expression of ACE2 receptors and TMPRSS2 proteases required for SARS-CoV-2 viral entry increases with age (Bunyavanich et al., 2020; Muus et al., 2021; Saheb Sharif-Askari et al., 2020; Schuler et al., 2020); this reduced expression may lead to decreased viral replication or lesser susceptibility to pulmonary infection. High viral load, however, is described in nasopharyngeal samples from children testing positive, even when asymptomatic (Aykac et al., 2021; Yonker et al., 2020). The presence of pre-existing, non-neutralizing antibodies to the common-cold human coronaviruses (HCoVs) HCoV-229E, -HKU1, -NL63, and -OC43, which could recognize SARS-CoV-2 early in infection, may either provide some level of protection in children or sustain inflammation in adults by increasing viral entry and innate responses in macrophages through Fc-γR-mediated entry (Ng et al., 2020; Perlman and Dandekar, 2005; Pierce et al., 2020). Finally, the question remains as to whether children mount a less-robust inflammatory response and, thus, have fewer, milder symptoms or, on the contrary, whether they mount a more efficient innate response and, thus, manage early control of viral replication.

Several reports have concluded, however, that the inflammatory response in children during COVID-19 is either undetectable or reduced as compared with adults (Felsenstein and Hedrich, 2020; Lu et al., 2020; Moratto et al., 2020). However, most studies examined innate response at a single time point, often relatively late after symptom onset, and were sometimes confounded by treatment, either of the children or of the adult comparators. In-depth, longitudinal analyses of early innate events after infection in children are challenging to obtain and is, thus, lacking.

Here, we report a detailed profiling of the immune response to SARS-CoV-2 in household clusters, from the onset of infection, including initial inflammatory antiviral responses, to its resolution in the 2 following months, and the generation of SARS-CoV-2-specific adaptive immunity. Responses in children and adult household members were compared in the context of mild COVID-19, the most common clinical presentation, and in the absence of any treatment. We found that children do indeed mount early, robust innate responses, but those resolve more rapidly than that found in adults. The rapid resolution does not, however, compromise the induction or quality of SARS-CoV-2-specific adaptive immunity, which is comparable with that seen in adults.

RESULTS

Similar viral load, despite fewer and more transient symptoms in children

Our longitudinal study was designed to follow-up contacts of recently diagnosed individuals to increase the chance of studying infection in the first days. Forty-six participants, index cases and their contacts, were included in these analyses. Thirty-seven had laboratory-confirmed SARS-CoV-2 infection; of which, 21 were adults (median age, 37 years; range, 20–62 years), and 16 were children, aged between 0.8 and 16 years (Figures 1A, 1B, and S1; Table S1). Patients were asked to report the date and nature of solicited COVID-19 symptoms; the kinetics of infection were divided into 5 time intervals according to the calculated days post onset of symptoms (DPOS; Figure 1A), with the earliest time point between 0 and 5 DPOS. Nine household contacts (5 adults, 4 children) remained negative by PCR and asymptomatic and, thus, served as negative controls followed for 2 weeks. The 16 infected children were distributed in 10 household clusters (C1 to C10), which held 12 infected adults, allowing paired comparisons between adults and children within the same cluster (Figures S2A and S2B). Participants were mainly white individuals, and comorbidities were reported in only a few of the infected adults (Table S1).

All SARS-CoV-2 infections were mild. Fewer symptoms, of shorter duration, were reported by children as compared with that of adults, either in their respective households or in other households (Figures 1C, 1D, and S2 for individual data). Among adults, some symptoms persisted for several weeks (anosmia, cough, and fatigue). Three children were totally asymptomatic and, there was no difference in any immunological and virological readouts presented in this study between those 3 asymptomatic children when compared with the symptomatic children. Those with the symptoms of longest duration were older, aged 14 and 16 years (Figure S2A).

At the time of diagnosis, viral load in nasopharyngeal swabs (NPSs) appeared similar among infected children and adults (Figure 1E), in line with other reports (Baggio et al., 2020; Colson et al., 2020; Heald-Sargent et al., 2020). Similar broad ranges of viral load (10^2 to 10^9 genome copies/mL) were also detected between inclusion and 18 DPOS (Figure 1F). There were no significant differences in viral clearance between adults and children, despite major differences in reported symptoms (Figure 1F). No other respiratory viruses were detected in NPSs.

Antiviral gene signature is robust in children and resolves more rapidly than it does in adults

The longitudinal expression of immune-related genes in peripheral blood revealed a common gene-expression signature in children and adults associated with SARS-CoV-2 infection (Figure 2). In the absence of a pre-exposure baseline, a first gene set was defined as all genes whose absolute change in expression was 1.5-fold more than the mean of all values of a patient for at least one time point. These genes were used for a blood transcriptional module (BTM; Li et al., 2014) analysis aimed at identifying which immune pathways were regulated. Heatmaps report genes belonging to the enriched BTMs and showed that, overall, the same gene clusters were found to be regulated in children and adults and that most changes occurred within the first 0–5 and 6–14 DPOS (Figure 2A). After 2 weeks, gene expression remained stable, indicative of a recovery phase. No changes in gene expression were observed in household contacts who remained PCR negative. Violin plots show selected, enriched BTMs (Figure 2B). Antiviral-interferon (IFN) signatures (such as M75, M127, and M150) and innate-cell activation (M67, M165, and M13) BTMs were prominent and upregulated at 0–5 DPOS. BTMs associated with stimulated CD4 T cell responses

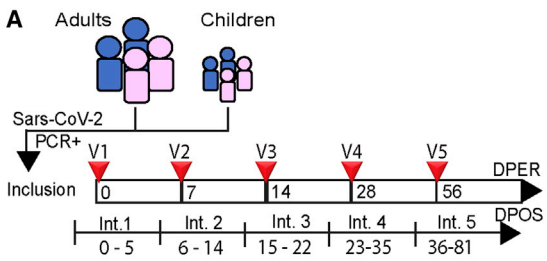

B

	Adults		Children	
	infected (PCR+)	negative (PCR-)	infected (PCR+)	negative (PCR-)
Number	21	5	16	4
Age (yr)	20 - 62	22 - 73	0.8 - 16	4 - 16
Gender (F/M)	(11/10)	(1/5)	(3/13)	(2/2)

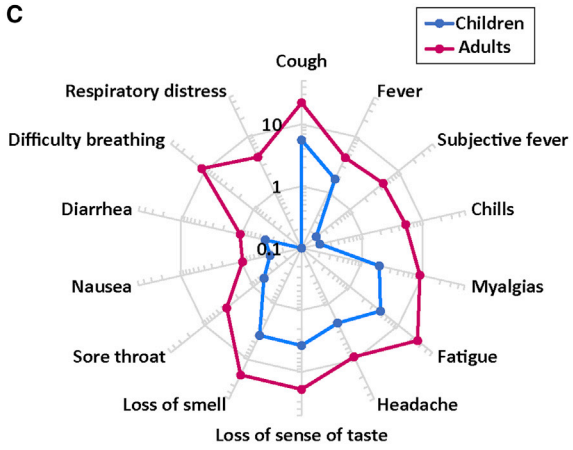

D

	Adults		Children	
	% with symptom	Duration (days)	% with symptom	Duration (days)
Cough	71.43	32.09	25.00	24.67
Fever	38.10	12.14	50.00	4.38
Subjective fever	33.33	18.40	12.50	1.50
Chills	57.14	10.00	12.50	1.50
Myalgias	80.95	11.73	18.75	9.67
Fatigue	85.71	34.86	37.50	12.00
Headache	85.71	11.33	56.25	4.56
Loss of sense of taste	71.43	29.50	12.50	28.00
Loss of smell	85.71	26.29	6.25	55.00
Sore throat	52.38	7.22	25.00	3.25
Nausea	23.81	4.75	18.75	1.67
Diarrhea	19.05	7.00	12.50	3.00
Difficulty breathing	23.81	58.00	0	0
Respiratory distress	4.76	90.00	0	0

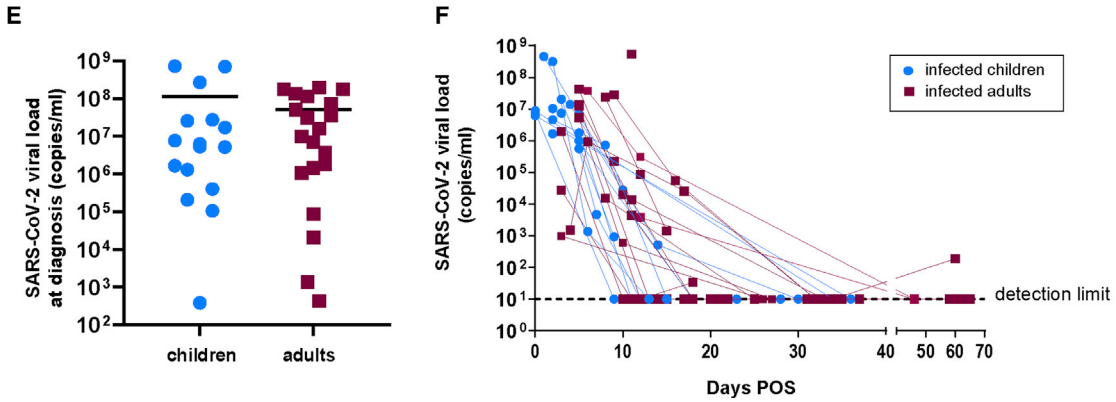

Figure 1. Children have fewer COVID-19 symptoms of shorter duration than adults do, despite a similar viral load

(A) Enrolled laboratory-confirmed patients with COVID-19 were scheduled for 5 visits at 0, 7, 14, 28, and 56 days post enrollment (DPER). Because the symptom onset may have occurred before or after the day of the positive PCR, the number of days post-onset of symptoms (DPOSs) is not equivalent to the number of days after enrollment. All patient samples fit in 5 intervals defined according to the calculated DPOS.

(B) For the analysis of the study population, the 46 participants were distributed into 4 groups by age (child versus adult) and PCR-confirmed COVID-19 status.

(C and D) The average duration of COVID-19-associated symptoms in infected children and adults represented by radial graphs (C), and the percentages of infected adults and children plus the average symptom duration in individuals presenting those symptoms (D).

(E and F) SARS-CoV-2 viral load by PCR (genome copies/mL) in nasopharyngeal samples in infected patients (16 children and 21 adults) at (E) diagnosis or (F) over time starting from first visit according to DPOS. Bars in graph (E) represent the mean.

(e.g., M4.5), plasma cells, and immunoglobulin (M156.0, M156.1, and M47.3) were upregulated in both age groups during the first 2 weeks POS, indicative of SARS-CoV-2-specific adaptive immune responses. During the course of the COVID-19 disease, we also observed changes in modules associated with platelet activation (M30), heme biosynthesis (M171), and erythrocyte differentiation (M173) (Figure S4).

To better compare gene expression between adults and children, we assessed differential gene expression, using the recovery time point (>5 weeks post symptom onset) as the baseline (Figures 3A–3D). Significantly up- or downregulated genes ($p < 0.05$ and abs(log_2-fold change [FC]) > 1.5) were then analyzed using BTMs. During the first 5 DPOS, there was significant upregulation of BTMs associated with antiviral IFN responses and

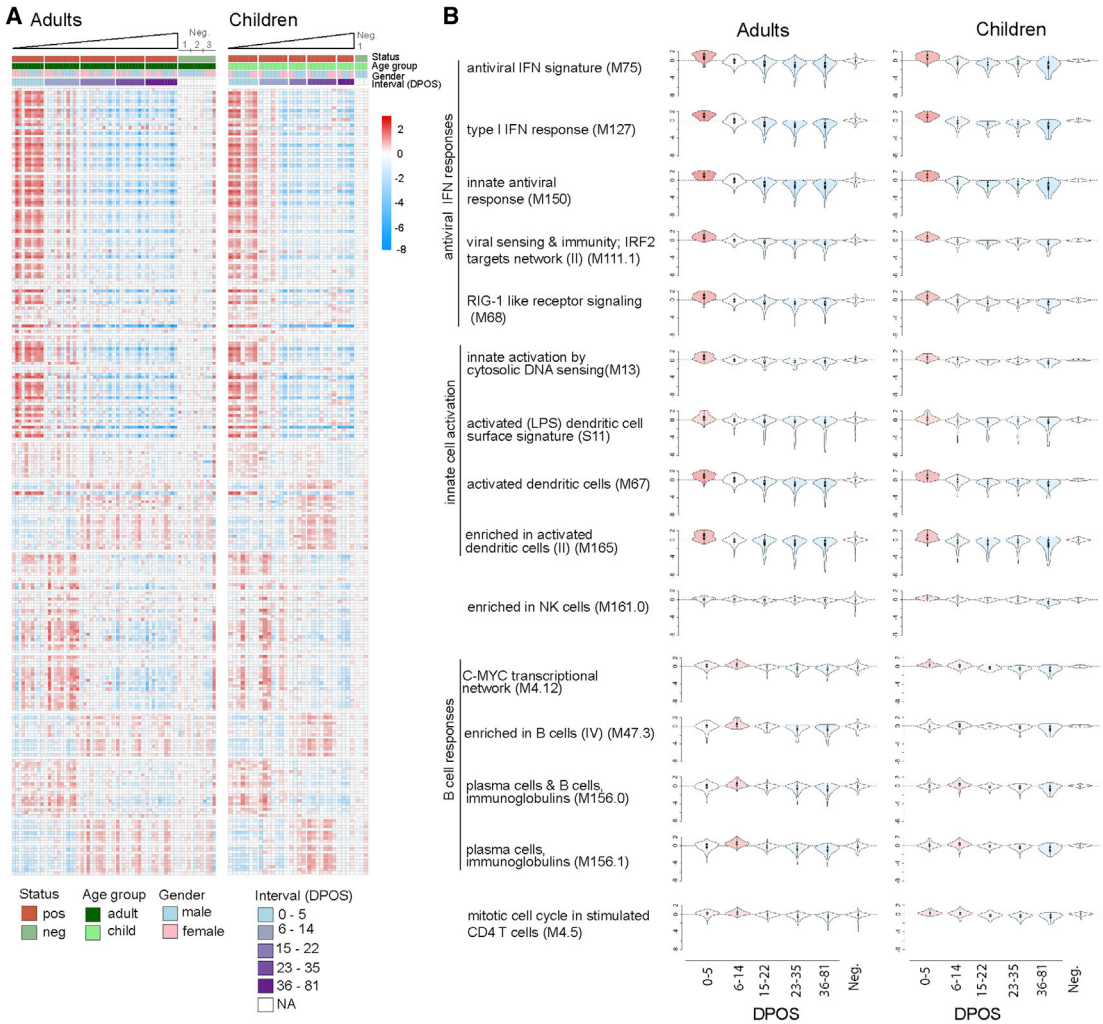

Figure 2. Mild COVID-19 induces a similar gene signature in the blood of adult and pediatric patients

(A) Heatmaps show changes in genes belonging to the enriched blood transcriptional modules (BTMs) over the course of COVID-19 in infected adults (n = 11) and children (n = 7).

(B) Violin plots show most of the enriched BTMs in the same patients. Colors reflect negative (blue) or positive (red) regulation. Repeated samples collected from healthy household contacts (3 adults and 1 child) at different time points have been included as negative controls (marked as Neg.). Data are from a single biological replicate.

Transcriptomic studies were performed by RNA-sequencing.

viral sensing (M127, M150, M75, and M111.1), immune-cell activation (e.g., activated dendritic cells [DCs]: M67 and M165), and inflammatory responses (complement activation [M112.0] and retinoic-acid-inducible gene 1 [RIG-1]-like receptor signaling [M68]) in both children and adults, in line with our previous analysis (Figure 3A). Upregulation of modules associated with natural killer (NK) cells (M61.0 and S1) was stronger in children in the first 5 DPOS (Figure 3A).

Although transcriptome changes had already subsided after 5 days in children, IFN antiviral responses and activated dendritic cells (M75, M150, M127, and M67) were maintained during the second week of disease in adults, subsiding only after 14 days (Figures 3B–3D). Unpaired analyses, including additional participants (with incomplete time courses), showed a similar pattern (Figure S4). Starting from the third week POS, modest changes (percentage of affected genes per module less than 25%) were observed in both age groups and were mainly associated with B cell responses. In children, the few upregulated modules at late time points were associated with E2F transcription factor network and regulation of signal transduction (Figures 3C and 3D).

Direct gene-expression comparisons between children and adults confirmed that innate inflammatory responses (IFN, DC activation, and cytokine responses) in adults were stronger and more persistent in the first 2 weeks POS. In contrast, BTMs specific for B cell responses were significantly overexpressed in children (Figures 3E and 3F). Altogether, the data show that children and adults had a similar innate response to SARS-CoV-2 but with a faster resolution in children.

Children's cytokine and innate-cell profiles share features of mild adult COVID-19 but have different kinetics and cell-activation status

Of 23 cytokines tested, statistically significant temporal changes in plasma CXCL10, granulocyte-macrophage colony stimulating factor (GM-CSF), interleukin 10 (IL-10), IL-1Rα, and IFN-α concentrations were observed in SARS-CoV-2-infected individuals (Figure 4). Although CXCL10 was significantly increased in the first week of disease in both children and adults, only adults maintained increased levels in the second week POS (Figure 4A), confirming our observations with IFN BTMs. Similar results were observed with GM-CSF (Figure 4B). Although some adults had higher plasma levels of CXCL10 and GM-CSF than children had, those differences were significant only at interval 2 (6–14 DPOS). Higher IL-10 levels were observed within the first 2 weeks POS in both age groups, although a significant difference compared with the latest time point was observed only in adults (Figure 4C). Higher levels of IL-1Rα early post-infection were observed in both children and adults, with adults having significantly higher levels at interval 2 (Figure 4D). Significantly higher levels of IFN-α early post-infection were observed in adults (Figure 4E)

The number and phenotype of circulating cells were analyzed on whole blood by flow cytometry. T and B lymphocyte counts were reduced in both age groups (Figures 5A and 5B) in the first week POS compared with that of late time points, but that reduction was more marked in children. Temporal changes in innate cells followed a similar pattern as previously reported in patients with COVID-19, irrespective of age. Numbers of $CD56^{bright}$NK cells (Figure 5C), DC subsets ($CD123^+$ plasmacytoid DCs [PDCs], $CD1c^+$ and $CD141^+$ myeloid DCs; Figures 5D–5F), $CD14^+$ monocytes and $CD16^+$ monocytes (Figures 5G and 5H), and $CD15^+$ neutrophils and basophils (Figures S5A and S5B) were low at 0–5 DPOS and slowly increased by recovery. By contrast, $CD14^+CD16^+$ monocyte counts were higher at 0–5 DPOS than they were at 36–81 DPOS (Figure 5I). Notable differences between infected children and adults included the tendencies for (1) greater fold changes in the highlighted cell levels in children, and (2) more transient changes (subsided at 6–14 DPOS in children versus 15–22 DPOS in adults) of $CD14^+CD16^+$ monocytes and $CD141^+$ DCs. Cell counts of these populations did not change over time in negative controls who were sampled at the same visit as infected contacts (Figure S5C). In addition, overall, significantly higher ($p < 0.05$) counts of lymphocytes (T, B, and NK cells) and DCs, especially PDCs, were found in children. Numbers of $CD141^+$ DCs ($p = 0.03$), $CD14^+CD16^+$ monocytes ($p = 0.05$), and basophils ($p = 0.02$) were significantly higher in children only at interval 2 (6–14 DPOS). Routine blood cell counts confirmed higher levels of lymphocytes in children and showed an early thrombocytopenia in adults, with platelet counts significantly lower ($p < 0.05$) than those in children at all time points (Figure S6).

The activation marker CD86 on monocyte and DC subsets was significantly upregulated shortly after symptom onset in all populations, with some children having relatively strong upregulation, especially in $CD14^+CD16^+$ monocytes (Figures 6 and S7A–S7C). Upregulation of CD86 expression on monocyte subsets and $CD1c^+$ DCs persisted within 6–14 DPOS only in adults (Figures 6B–6G). Changes in human leukocyte antigen-DR isotype (HLA-DR) expression were also observed, with upregulation in $CD14^+$ and $CD16^+$ monocytes shortly after SARS-CoV-2 infection in both age groups (Figures S7D and S7E) and downregulation in $CD1c^+$ DCs. Children had significantly higher HLA-DR levels in $CD1c^+$ DCs than adults had, up to 22 DPOS (Figure S7F). Consistent with the mild disease presentation in our cohort, we did not detect decreased HLA-DR expression in $CD14^+CD16^+$ monocytes, which is thought to be a predictor of severe disease (Mudd et al., 2020; Wei et al., 2020). In line with the cell numbers, there was no change in the surface expression of activation markers in non-infected individuals (Figure S7G).

Overall, all children could mount an innate-immune response to SARS-CoV-2 as robust as that in adults, but the response resolved faster in children.

Lower pre-existing humoral immunity to common-cold HCoVs in children

At the first visit, no immunoglobulin G (IgG) antibodies to the S1 domain of the SARS-CoV-2 spike antigen were detected in our study population (Figure 7A). In contrast, IgGs specific to S1 of the other four HCoVs were detected at the first visit, indicating previous exposure. S1 HCoV-specific IgGs were significantly lower in children than they were in adults for both beta coronaviruses HCoV-HKU1 and HCoV-OC43 (Figures 7B and 7C) and alpha coronaviruses HCoV-229E and HCoV-NL63 (Figures S8A and S8B).

Differences in innate-response kinetics between age groups do not affect the quality of SARS-CoV-2-specific adaptive responses

Differences in the persistence and level of monocyte and DC activation may lead to quantitative and functional changes in SARS-CoV-2-specific adaptive responses. SARS-CoV-2-specific neutralizing activities and memory B cells were, however, detected at similar levels in both infected children and adults for up to 5 weeks POS (Figures 7D and 7E). IgG responses predominated, and similar levels of receptor-binding domain (RBD)- and S-specific IgG1 and IgG3 isotypes were measured in both age groups (Figures 7F–7H and S8C–S8E). SARS-CoV-2-specific IgG2 and IgG4 isotypes were not detected (data not shown). The antibody-dependent complement deposition (ADCD; Figures 7I and S8F) and antibody-dependent cellular phagocytosis (ADCP; Figure S8G) activation capacity of SARS-CoV-2-specific antibodies for both RBD and S similarly increased with time in adults and children. There was a trend toward more-rapid antibody induction in children for anti-RBD IgG, IgG1, and ADCD function, in line with the earlier increase in the expression of genes associated with B cell activation as compared with adults. In contrast to what has been recently reported (Weisberg et al., 2021), children mounted an antibody response to N as efficiently as adults did (Figure 7J). Interestingly, adults tended to have more N-specific antibodies in the first 5 DPOS, in line with the presence of potentially cross-reactive antibodies to HCoVs.

Overall, in our study, children had a similar level and profile of SARS-CoV-2-specific antibody levels compared with that of adults with mild COVID-19, despite having fewer symptoms and less-persistent antiviral innate responses.

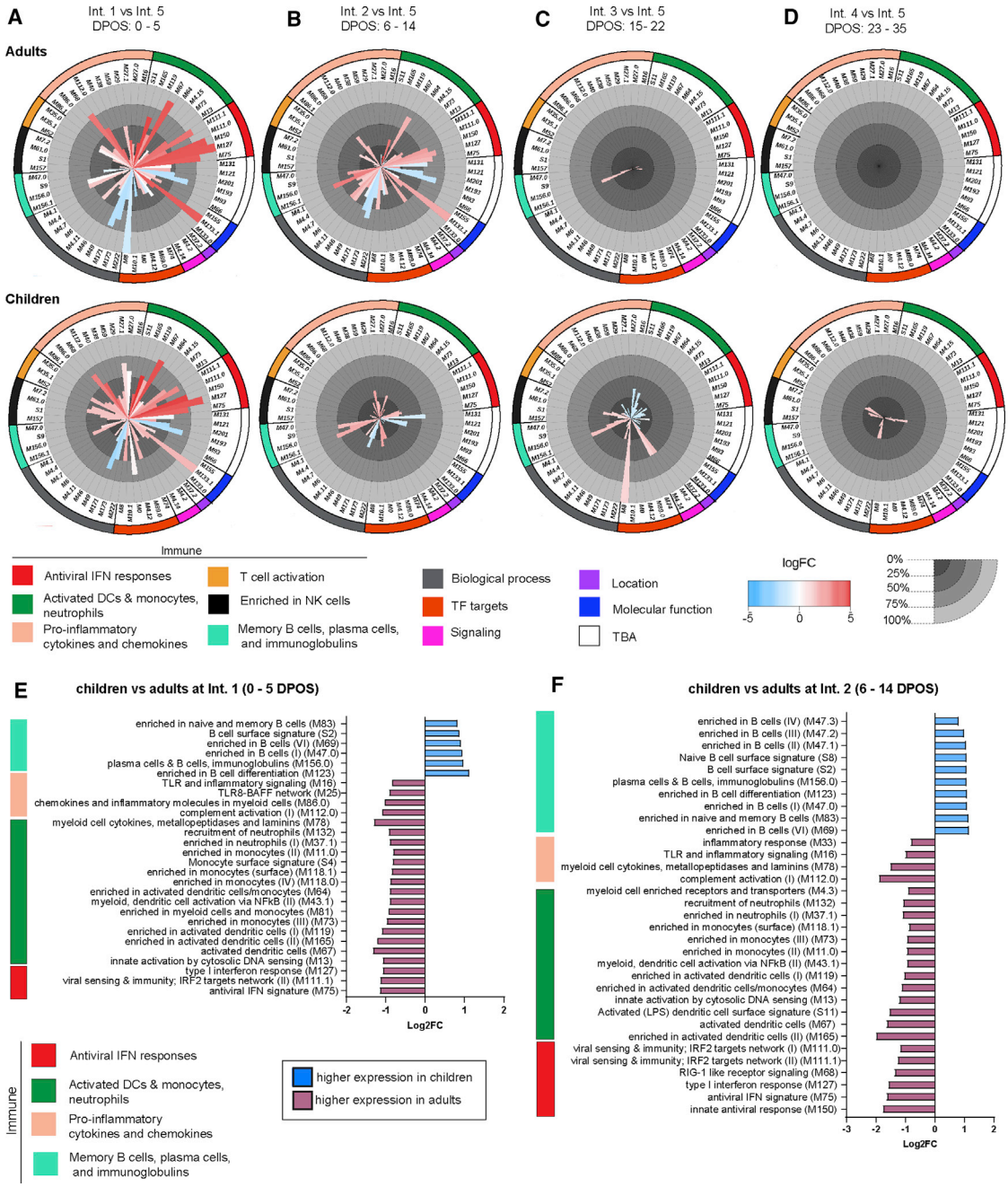

Figure 3. Innate inflammatory responses induced by SARS-CoV-2 resolve within a week post onset of symptoms in children only

(A–D) Star graphs show BTM analyses performed by using the differential expressed genes (DEGs) that emerged from the following paired comparisons in adults (n = 9) and children (n = 5): (A) interval 1 versus 5, (B) interval 2 versus 5, (C) interval 3 versus 5, and (D) interval 4 versus 5. Graphs report the averaged log_2FC of the DEGs belonging to each BTM, as well as the percentage of BTM genes being differentially expressed. BTMs with less than 25% DEGs in all 8 comparisons have been excluded from graphs; BTMs belonging to the same category have been grouped and assigned the same color code, except for BTMs belonging to the immune category, which have been arbitrarily grouped in sub-categories to help data interpretation.

(E and F) Bar graphs show BTM analysis performed by using the DEGs emerged from the following unpaired comparisons: (E) children (n = 8) versus adults (n = 10) at interval 1, and (F) children (n = 8) versus adults (n = 11) at interval 2. Graphs report only enriched BTMs belonging to the immune category, with at least 25% of DEGs, and the averaged log_2FC of the DEGs belonging to each BTM ≥ 0.8 or ≤ -0.8. Data are from a single biological replicate.

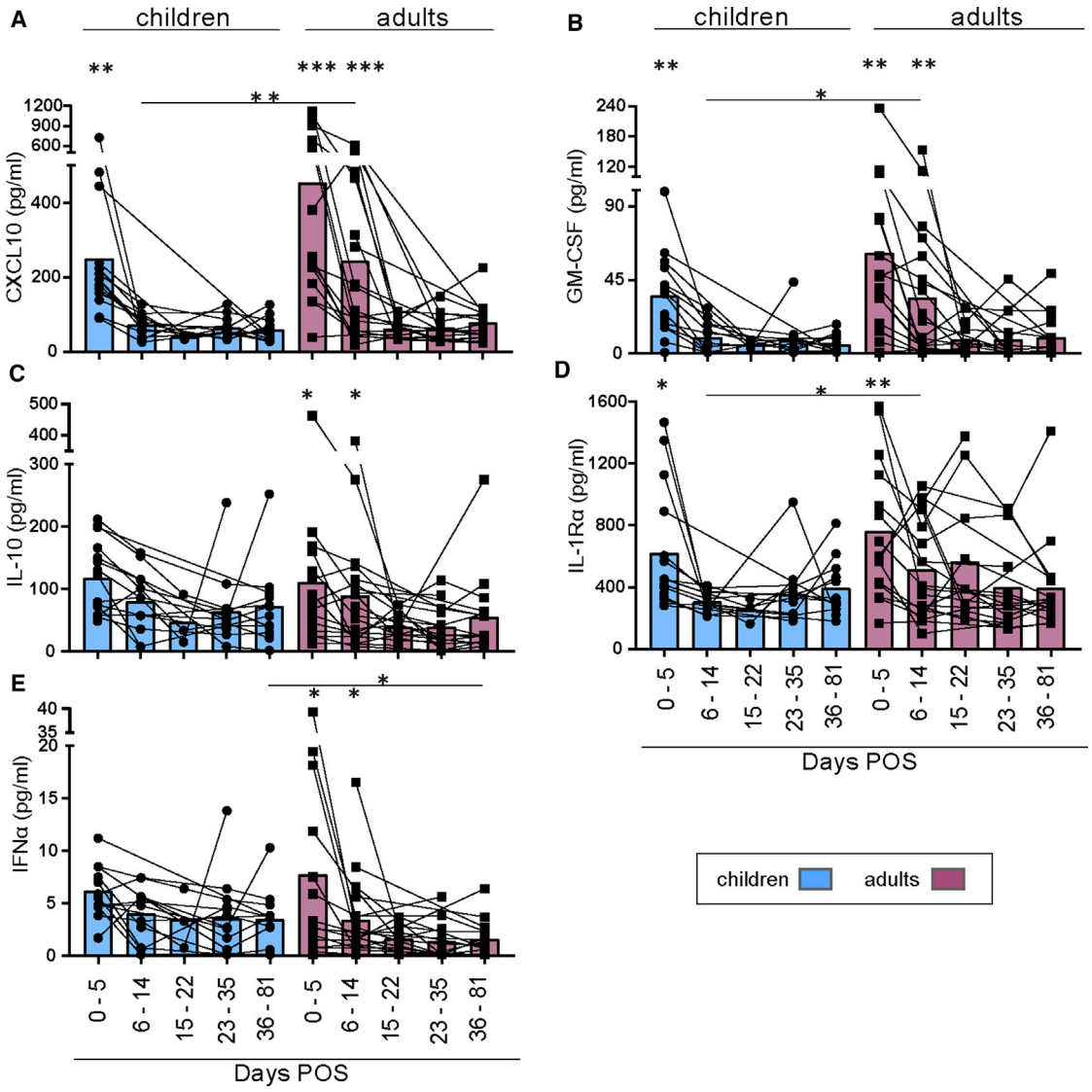

Figure 4. Longitudinal changes of pro-inflammatory cytokines in plasma of adult and pediatric patients

(A–E) Plasma concentration of (A) CXCL10, (B) GM-CSF, (C) IL-10, (D) IL-1Rα, and (E) IFN-α in children (filled circles, n = 16), and adults (filled squares, n = 20) over time, according to DPOS. Data are from a single biological replicate. Bars represent the mean. For each patient, early responses at interval 1 (0–5 DPOS) and 2 (6–14 DPOS) have been compared with responses at the latest time point available using a paired t test. For comparisons of children versus adults, we used the Mann-Whitney U test. *p < 0.05, **p < 0.01, ***p < 0.001.

DISCUSSION

These results demonstrate that children mount potent antiviral innate responses, similar in amplitude to those of adults with mild COVID-19; however, those responses are significantly different in duration: the transience of innate responses in children may explain this population's limited symptomatology. We identified, in both age groups, a typical innate signature, characterized by early IFN responses; an increase in cytokines, such as CXCL10 and GM-CSF; transient lymphopenia; and an increase in activated monocytes and DCs. The rapid resolution of inflammation in children, however, was striking. IFN-stimulated genes, cytokines, and cell activation were seen only in the first 5 DPOS in children, whereas they persisted in adults. Children had no SARS-CoV-2 antibodies during that period, making it unlikely that they could have been infected earlier than adults were. In addition, during the study period, most transmission likely occurred from adult to pediatric contacts (Stringhini et al., 2020). Severe COVID-19 is associated with a lower initial IFN response, followed by an uncontrolled and persistent inflammatory response (Zhang et al., 2020), and the rapidity of the resolution of inflammation determines the disease trajectory (Lucas et al., 2020). Thus, we propose that efficient early IFN responses and a rapid return to homeostasis contribute to protect children from COVID-19-associated symptoms. Conversely, persistent IFN is known to be associated with

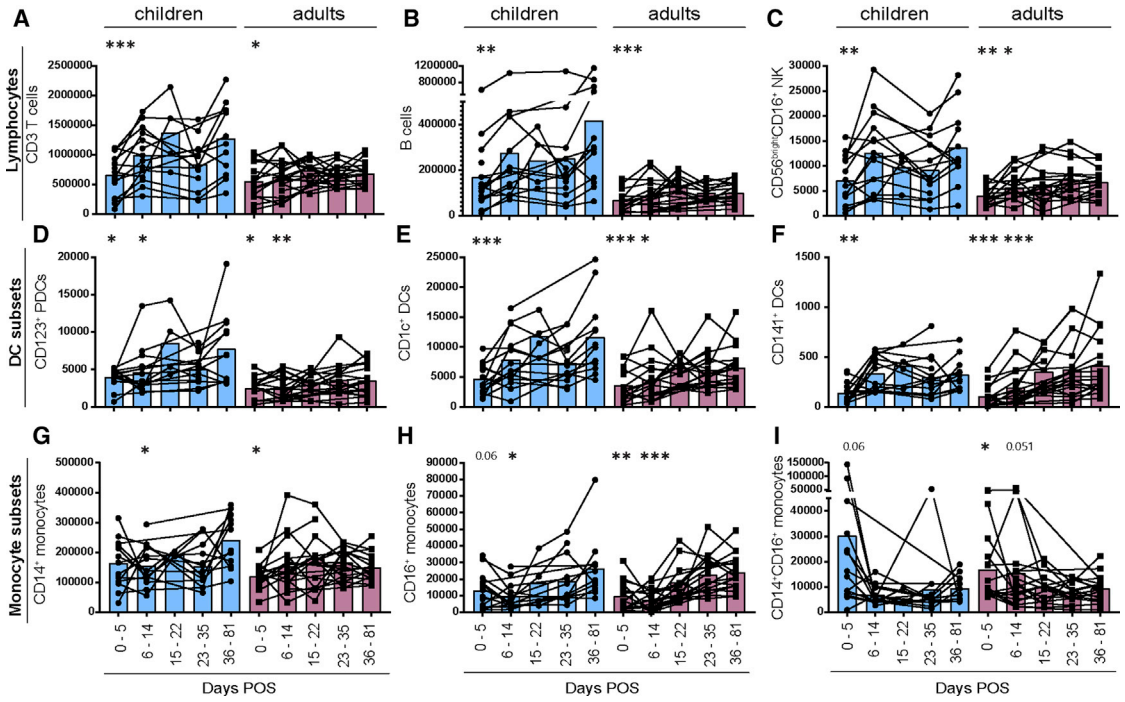

Figure 5. Longitudinal cellular immune profiling in whole blood of pediatric and adult patients

(A–I) Normalized numbers of major immune cell populations in whole blood of children (filled circles, n = 16), and adults (filled squares, n = 20) during the course of COVID-19 disease: (A) CD3 T cells, (B) B cells, (C) $CD56^{bright}$ NK cells, (D) plasmacytoid DCs (PDCs), (E) myeloid $CD1c^+$ DCs, (F) myeloid $CD141^+$ DCs, (G) classical $CD14^+$ monocytes, (H) $CD16^+$ monocytes, and (I) intermediate $CD14^+CD16^+$ monocytes. Data are from a single biological replicate. Bars represent the mean. For each patient, early responses at interval 1 (0–5 DPOS) and 2 (6–14 DPOS) have been compared with responses at the latest time point available using a paired t test: *$p < 0.05$, **$p < 0.01$, ***$p < 0.001$. For comparisons of children versus adults, we used the Mann-Whitney U test, and p values are shown in the text.

deleterious effects for the host, as a driver of detrimental immunopathology (Dagenais-Lussier et al., 2017), which could explain the longer duration and intensity of symptoms in adults with mild COVID-19.

The exact mechanism leading to better and faster disease resolution in children remains unclear. Baseline cytokine level is generally lower in children (Decker et al., 2017) and the lungs of children suffering from acute respiratory distress syndrome are less inflamed than those of adults (Schouten et al., 2019). Recurrent infections in childhood may lead to a specific state of higher innate responsiveness to viruses, potentially through a trained immunity phenomenon (Divangahi et al., 2021). Interestingly, robust innate responses, in particular strong IFN responses, are associated with better outcomes after influenza and RSV infection (Heinonen et al., 2020). Nevertheless, children are, in general, more susceptible to respiratory infections to which they develop more symptoms. SARS-CoV-2, like SARS-CoV-1, appears to specifically dampen IFN responses, which may explain why a similar pattern of pauci-symptomatic disease has also been reported for SARS-CoV-1 in pediatric patients (Aleebrahim-Dehkordi et al., 2021).

Early studies reported no major leukocyte aberrations and limited inflammatory responses in children (Henry et al., 2020), whereas we observed significant changes at the cellular level and an increase of CXCL10 and GM-CSF. It is possible that peak responses were missed in previous studies because our study shows that they occur very early and only transiently. Other groups have reported similar cytokine levels in hospitalized pediatric patients as compared with that of adults who did not require ventilation, except for higher levels of IL-17 and INF-γ (Pierce et al., 2020). We did not find a specific increase in IL-17 or IFN-γ in our longitudinal analysis, so that may be a feature of more-severe disease. Although lymphopenia was mainly reported in severe cases of pediatric COVID-19 (Wu et al., 2020), it is likely to also occur during mild disease, as shown in our cohort. In line with our data, Neeland et al. (2021) have also reported a potent innate response in children with mild COVID-19. We found a similar reduction in NK cells and all monocyte and DC subsets in the acute phase, except for $CD14^+CD16^+$ monocyte numbers, which were increased in our pediatric cohort. That discrepancy may be due to differences in the early time point between the two studies. Interestingly, Neeland et al (2021) also highlighted higher activation of neutrophils in children, which were also strongly reduced in numbers in our cohort, highlighting a potential role for neutrophils in the early control of infection.

We had presumed that inflammatory responses to SARS-CoV-2 would drive the patterns and intensity of inflammatory symptoms. The intensity of innate responses did not, however, correlate with symptom severity or age but, apparently, merely reflected the presence of virus in the upper respiratory tract. The question remains whether this local response is more

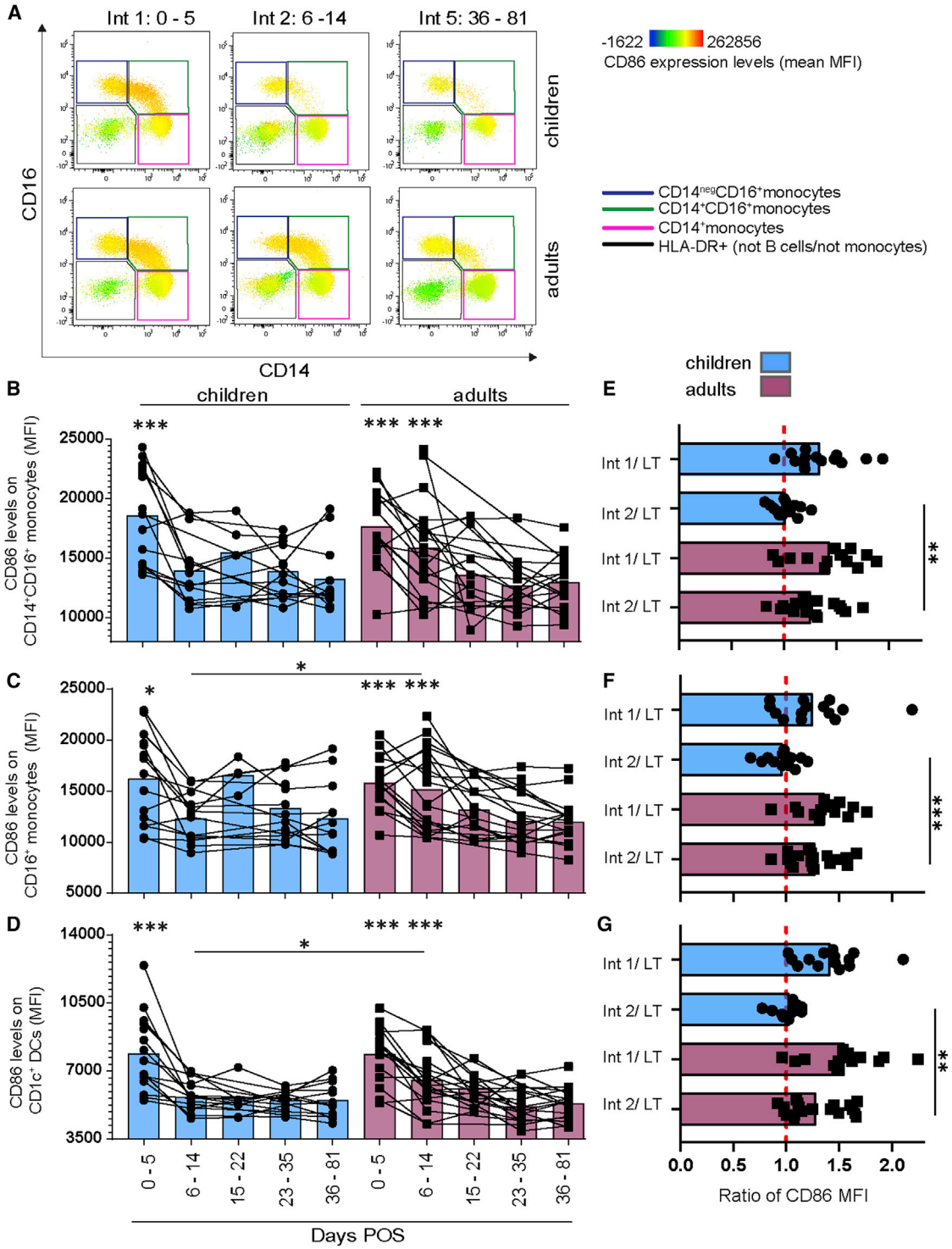

Figure 6. Activation status of DC and monocyte subsets in blood of children and adults during the course of COVID-19

(A) Flow cytometry dot plots show CD86 expression levels on distinct monocyte subsets at early time points after infection (interval 1, 0–5 DPOS; interval 2, 6–14 DPOS), and at a late time point (interval 5, 36–81 DPOS) from representative pediatric and adult patients.

(B–D) Bar graphs show mean fluorescence intensity (MFI) values of CD86 on (B) $CD14^+CD16^+$ monocytes, (C) $CD16^+$ monocytes, and (D) $CD1c^+$ DCs. Bars represent the mean. For each patient (20 adults and 16 children), early responses at intervals 1 and 2 have been compared with responses at the latest time point available using a paired t test. For comparisons of children versus adults, we used the Mann-Whitney U test. *$p < 0.05$, **$p < 0.01$, ***$p < 0.001$.

(legend continued on next page)

efficient at eliminating the virus. A recent study showed that children, as compared with adults have a more-potent innate response in the nasal cavity, characterized by a greater anti-viral response, including IFN-γ and IFN-α, suggesting that they are better equipped than adults are to control the virus replication early during the infection (Pierce et al., 2021). In line with that finding, some of the children in our study had greater innate activation than that of the average adults with mild COVID-19. Children have higher numbers of lymphocytes, which may contribute to better disease control (Erkeller-Yuksel et al., 1992; Vakkila et al., 2004; Valiathan et al., 2016). Given that circulating T, B, and NK cells decrease post-infection, it is tempting to speculate that they can be recruited earlier and in higher numbers at the site of infection to clear it faster than adults can. That hypothesis is in line with the observation of stronger upregulation of BTMs associated with NK cells in children in the first 5 DPOS. Plasmacytoid DC numbers during infancy have been inversely associated with childhood respiratory-tract infections and wheezing (Upham et al., 2009), and in our study, children had more circulating PDCs than adults had; their role in infection control in children should, thus, be further evaluated.

Another important difference was the lower level of baseline antibodies against HCoVs in children, in line with another recent report (Pierce et al., 2021). In adults, higher levels of pre-existing binding, but non-neutralizing, antibodies to HCoVs may bind to the virus, enhancing viral entry into macrophages or DCs through FcR-mediated binding and increase or prolong inflammation. In contrast to SARS-CoV-1 (Iwasaki and Yang, 2020; Jaume et al., 2011; Yip et al., 2014), recent *in vitro* data using monocyte-derived macrophages suggest that this antibody-dependent enhancement mechanism may not be operating with SARS-CoV-2 (Zheng et al., 2021). Overall, the role of pre-existing and potentially cross-reactive HCoVs-specific antibodies in age-dependent susceptibility to SARS-CoV-2 is not supported by the current evidence (Anderson et al., 2021).

Finally, the difference observed in the kinetics and nature of the innate response does not seem to influence the quality and magnitude of the SARS-CoV-2-specific antibody response after mild COVID-19. In contrast to a recent report by Weisberg et al. (2021), we and others (Bartsch et al., 2021; Goenka et al., 2021; Selva et al., 2021) have found similar levels of neutralizing antibody and a similar breadth of response against different SARS-CoV-2 antigens, including against the nucleocapsid. Individuals who recover rapidly from symptomatic COVID-19 have been shown to have more-sustained antibody production and increased somatic mutations in memory B cells (Chen et al., 2020). Children with more neutralizing antibodies and specific plasmablasts 7 days after disease onset had lower viral load (Cotugno et al., 2021). B cell activation may, therefore, occur faster in children. Interestingly, we observed that BTM associated with B cell response and immunoglobulins were more rapidly stimulated in children, in line with the trend for more-rapid production of antibodies specific to RBD. Although requiring confirmation in a larger cohort, this finding would further support the notion that B cell stimulation and, thereby, antibody production are particularly efficient in children, who resolve inflammation and symptoms more rapidly than adults do. Thus, provided that antibodies are directly involved in protection, children could be similarly protected as adults from SARS-CoV-2 reinfection, despite their pauci- or asymptomatic primary infections.

Our study had several limitations, chief among them its observational design and its relatively small size. All patients had mild COVID and, therefore, our data cannot be extrapolated to more-severe disease. Differences in symptom profiles between adults and children meant that we could not match their profiles for direct comparisons.

In conclusion, our data suggest that the fewer symptoms of shorter duration in children may reflect their more rapid resolution of innate responses to SARS-CoV-2.

STAR★METHODS

Detailed methods are provided in the online version of this paper and include the following:

- KEY RESOURCES TABLE
- RESOURCE AVAILABILITY
  - Lead contact
  - Materials availability
  - Data and code availability
- EXPERIMENTAL MODEL AND SUBJECT DETAILS
  - Setting, study population, and design
- METHODS DETAILS
  - SARS-CoV-2 RNA quantification
  - RNA-sequencing of whole blood
  - RNA-sequencing data analysis
  - Cytokine measurement in plasma
  - Blood cell phenotyping by flow cytometry
  - Analysis of antibody response
  - Neutralization assay (sVNT)
  - IgG antibodies to human coronaviruses (HCoVs) determined by protein microarray
  - Memory B cell analysis by enzyme-linked immunospot (ELISpot) assay
- QUANTIFICATION AND STATISTICAL ANALYSIS

SUPPLEMENTAL INFORMATION

Supplemental information can be found online at https://doi.org/10.1016/j.celrep.2021.109773.

ACKNOWLEDGMENTS

We thank Kinga K. Smolen for technical advice; Barbara Lemaitre, Gianna Cadau, Mario Valenti, Chantal Tougne, Paola Fontannaz, Loïck Staudenmann, Irene Sabater Royo, Floriane Auderset, Pascale Sattonnet, and Manel Essaidi for their contributions to processing the clinical samples and experimental work; the colleagues at the fluorescence-activated call sorting (FACS) facility at the University of Geneva; the iGE3 Genomics platform of the University of Geneva for RNA sequencing (RNA-seq) data generation and assistance; the

(E–G) Horizontal bar graphs show the mean ratio of CD86 MFI values at early time points, interval (Int.) 1 or Int. 2, to the latest time point available (LT) belonging to Int 5 or Int. 4 for (E) $CD14^{+}CD16^{+}$ monocytes, (F) $CD16^{+}$ monocytes, and (G) $CD1c^{+}$ DCs; Mann-Whitney U test; *$p < 0.05$, **$p < 0.01$, ***$p < 0.001$. Int. 1/LT, 14 adults, 14 children; int. 2/LT, 19 adults, 14 children. Data are from a single biological replicate.

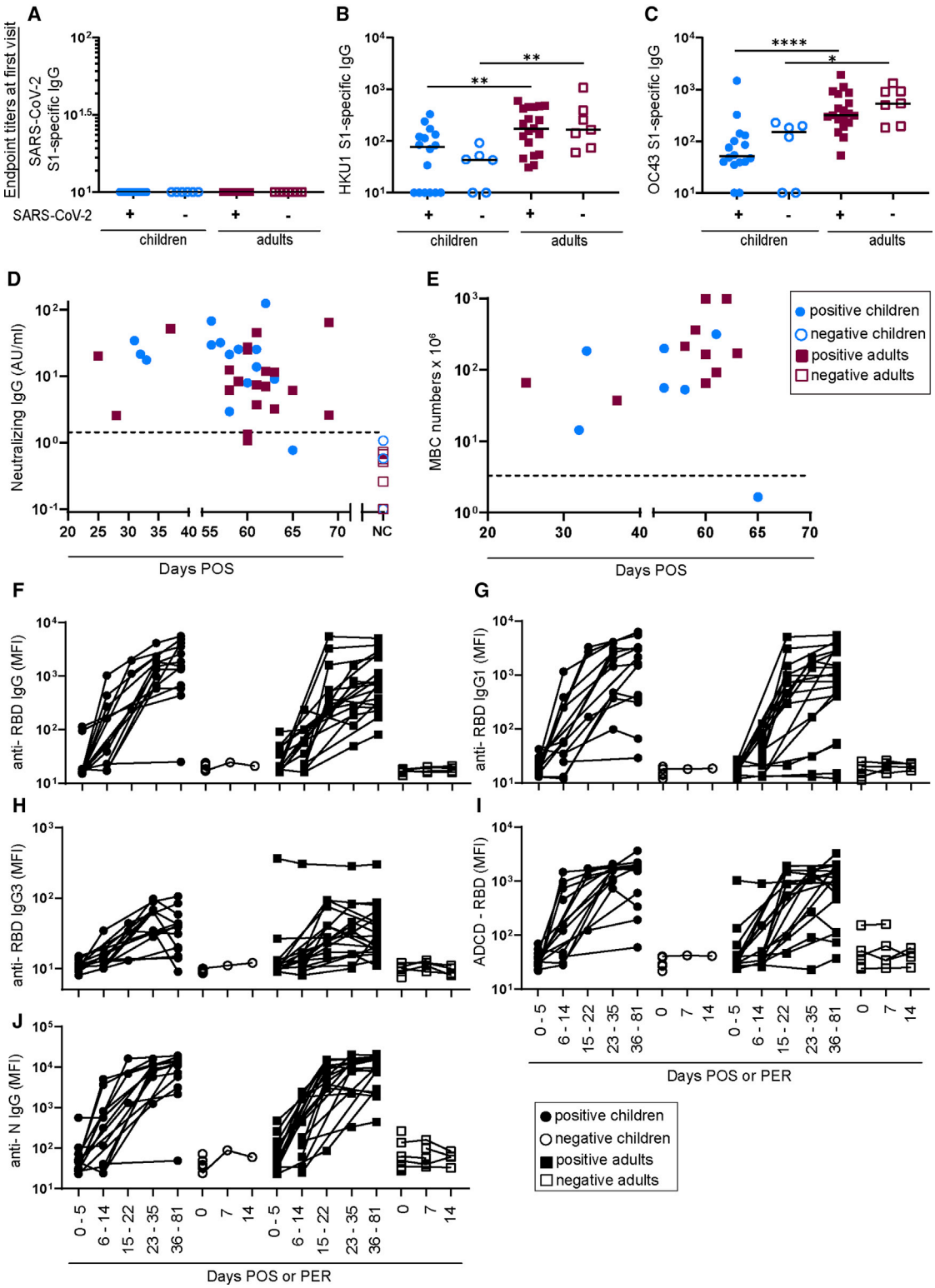

Figure 7. Adults have more pre-existing IgG antibodies to HCoVs than children have but similar antibody and MBC responses to SARS-CoV-2

(A–C) Endpoint titers specific to S1 from (A) SARS-CoV-2, (B) HCoV-HKU1, and (C) HCoV-OC43 in sera collected at the first visit (V1) in SARS-CoV-2 infected (+) individuals (19 adults, 16 children) or their SARS-CoV-2 PCR^{neg} (−) contacts (6 children and 7 adults). Bars represent the median value. Mann-Whitney U test; *$p < 0.05$, **$p < 0.01$, ****$p < 0.0001$.

(legend continued on next page)

Clinical Trials Unit of the Geneva University Hospitals and Faculty of Medicine for nursing and administrative support; Elodie von Dach for setting up the study infrastructure and data collection; and Diego Andrey, Adrien Calame, Lena Mazza, Cecilia Schweblin, and Mathilde Bellon for their involvement in patient recruitment and sample collection. We thank Paul-Henri Lambert for his critical review of the manuscript, Dr. Matthew Morgan for editorial assistance, and Dirk Eggink and Johan Reimerink for critical discussions and support. We are grateful to all volunteers of the "Understanding COVID study" and the healthy control group for their participation in the study. This work was supported by the Swiss National Science Foundation (grant number 31CA30_196732/1 to C.-A.S.), the HUG Private Foundation, and the Pictet Charitable Foundation. A.M.D. is supported by the Giorgi-Cavaglieri Foundation.

AUTHOR CONTRIBUTIONS

M.V., A.H., P.M.-M., B.M., L.K., I.E., C.S.E., G.B.-R., A.M.D., and C.-A.S. conceived the study and wrote the clinical protocol. M.V. analyzed most of the clinical data, conducted and analyzed the cellular immunity studies, and extracted and quantified RNA for RNA-seq analyses. A.H. organized, coordinated, and supervised the clinical study. S.L. performed RNA-seq data analysis and generated related figures. P.M.-M. performed the Luminex assay for cytokine detection and data analysis and the memory B cell assay together with C.S.E. B.M. generated and analyzed the neutralization antibody data. S.B. performed complementary statistical analyses. C.A. and F.P.-R. quantified the virus in all clinical samples. S.S., A.T., and A.M. performed isotype and subclass analyses, ADCD, and ADCP assays. G.-J.G. and C.R. measured IgG antibodies to human coronaviruses by protein microarray. A.H., N.L., and G.B.-R. recruited participants, organized and conducted study visits, and collected clinical specimens. M.V. and A.M.D. prepared figures and wrote the manuscript. All authors provided intellectual input and reviewed the manuscript.

DECLARATION OF INTERESTS

All authors declare no competing interests.

Received: February 18, 2021
Revised: June 25, 2021
Accepted: September 7, 2021
Published: October 5, 2021

REFERENCES

Ackerman, M.E., Moldt, B., Wyatt, R.T., Dugast, A.S., McAndrew, E., Tsoukas, S., Jost, S., Berger, C.T., Sciaranghella, G., Liu, Q., et al. (2011). A robust, high-throughput assay to determine the phagocytic activity of clinical antibody samples. J. Immunol. Methods *366*, 8–19.

Aleebrahim-Dehkordi, E., Soveyzi, F., Deravi, N., Rabbani, Z., Saghazadeh, A., and Rezaei, N. (2021). Human coronaviruses SARS-CoV, MERS-CoV, and SARS-CoV-2 in children. J. Pediatr. Nurs. *56*, 70–79.

Anderson, E.M., Goodwin, E.C., Verma, A., Arevalo, C.P., Bolton, M.J., Weirick, M.E., Gouma, S., McAllister, C.M., Christensen, S.R., Weaver, J., et al.; UPenn COVID Processing Unit (2021). Seasonal human coronavirus antibodies are boosted upon SARS-CoV-2 infection but not associated with protection. Cell *184*, 1858–1864.e10.

Aykac, K., Cura Yayla, B.C., Ozsurekci, Y., Evren, K., Oygar, P.D., Gurlevik, S.L., Coskun, T., Tasci, O., Demirel Kaya, F., Fidanci, I., et al. (2021). The association of viral load and disease severity in children with COVID-19. J. Med. Virol. *93*, 3077–3083.

Baggio, S., L'Huillier, A.G., Yerly, S., Bellon, M., Wagner, N., Rohr, M., Huttner, A., Blanchard-Rohner, G., Loevy, N., Kaiser, L., et al. (2020). SARS-CoV-2 viral load in the upper respiratory tract of children and adults with early acute COVID-19. Clin. Infect. Dis. *73*, 148–150.

Bartsch, Y.C., Wang, C., Zohar, T., Fischinger, S., Atyeo, C., Burke, J.S., Kang, J., Edlow, A.G., Fasano, A., Baden, L.R., et al. (2021). Humoral signatures of protective and pathological SARS-CoV-2 infection in children. Nat. Med. *27*, 454–462.

Brodin, P. (2020). Why is COVID-19 so mild in children? Acta Paediatr. *109*, 1082–1083.

Bunyavanich, S., Do, A., and Vicencio, A. (2020). Nasal gene expression of angiotensin-converting enzyme 2 in children and adults. JAMA *323*, 2427–2429.

Castagnoli, R., Votto, M., Licari, A., Brambilla, I., Bruno, R., Perlini, S., Rovida, F., Baldanti, F., and Marseglia, G.L. (2020). Severe acute respiratory syndrome coronavirus 2 (SARS-CoV-2) infection in children and adolescents: a systematic review. JAMA Pediatr. *174*, 882–889.

Chen, Y., Zuiani, A., Fischinger, S., Mullur, J., Atyeo, C., Travers, M., Lelis, F.J.N., Pullen, K.M., Martin, H., Tong, P., et al. (2020). Quick COVID-19 healers sustain anti-SARS-CoV-2 antibody production. Cell *183*, 1496–1507.e16.

Colson, P., Tissot-Dupont, H., Morand, A., Boschi, C., Ninove, L., Esteves-Vieira, V., Gautret, P., Brouqui, P., Parola, P., Lagier, J.C., et al. (2020). Children account for a small proportion of diagnoses of SARS-CoV-2 infection and do not exhibit greater viral loads than adults. Eur. J. Clin. Microbiol. Infect. Dis. *39*, 1983–1987.

Consiglio, C.R., Cotugno, N., Sardh, F., Pou, C., Amodio, D., Rodriguez, L., Tan, Z., Zicari, S., Ruggiero, A., Pascucci, G.R., et al.; CACTUS Study Team (2020). The immunology of multisystem inflammatory syndrome in children with COVID-19. Cell *183*, 968–981.e7.

Corman, V.M., Landt, O., Kaiser, M., Molenkamp, R., Meijer, A., Chu, D.K., Bleicker, T., Brünink, S., Schneider, J., Schmidt, M.L., et al. (2020). Detection of 2019 novel coronavirus (2019-nCoV) by real-time RT-PCR. Euro Surveill. *25*, 2000045.

Cotugno, N., Ruggiero, A., Bonfante, F., Petrara, M.R., Zicari, S., Pascucci, G.R., Zangari, P., De Ioris, M.A., Santilli, V., Manno, E.C., et al.; CACTUS Study Team (2021). Virological and immunological features of SARS-CoV-2-infected children who develop neutralizing antibodies. Cell Rep. *34*, 108852.

Dagenais-Lussier, X., Loucif, H., Murira, A., Laulhé, X., Stäger, S., Lamarre, A., and van Grevenynghe, J. (2017). Sustained IFN-I expression during established persistent viral infection: a "bad seed" for protective immunity. Viruses *10*, 12.

Decker, M.L., Grobusch, M.P., and Ritz, N. (2017). Influence of age and other factors on cytokine expression profiles in healthy children—a systematic review. Front Pediatr. *5*, 255.

Divangahi, M., Aaby, P., Khader, S.A., Barreiro, L.B., Bekkering, S., Chavakis, T., van Crevel, R., Curtis, N., DiNardo, A.R., Dominguez-Andres, J., et al. (2021). Trained immunity, tolerance, priming and differentiation: distinct immunological processes. Nat. Immunol. *22*, 2–6.

(D) Viral neutralizing titers in serum samples of infected adults (n = 20) and children (n = 15) at the latest time point available; negative contacts (NC; 7 adults, 6 children) served as control.
(E) S1-specific memory-B cell numbers (per million of plated peripheral blood mononuclear cells [PBMCs]) in infected patients at the latest time point available (10 adults; 7 children).
(F–J) RBD-specific (F) IgG, (G) IgG1, and (H) IgG3 antibody levels in serum samples (captured by MFI measurements in a Luminex assay). (I) RBD-specific antibody-dependent complement deposition (ADCD) activity (captured MFI measurements of C3 deposition) in serum samples. (J) Nucleocapsid (N)-specific IgG antibodies. Serum samples of infected adults (n = 19) and children (n = 16), and their negative contacts (6 children and 7 adults) were tested. Data are from a single biological replicate. PER, post enrollment for negative controls.

Dobin, A., Davis, C.A., Schlesinger, F., Drenkow, J., Zaleski, C., Jha, S., Batut, P., Chaisson, M., and Gingeras, T.R. (2013). STAR: ultrafast universal RNA-seq aligner. Bioinformatics *29*, 15–21.

Erkeller-Yuksel, F.M., Deneys, V., Yuksel, B., Hannet, I., Hulstaert, F., Hamilton, C., Mackinnon, H., Stokes, L.T., Munhyeshuli, V., Vanlangendonck, F., et al. (1992). Age-related changes in human blood lymphocyte subpopulations. J. Pediatr. *120*, 216–222.

Felsenstein, S., and Hedrich, C.M. (2020). SARS-CoV-2 infections in children and young people. Clin. Immunol. *220*, 108588.

Fischinger, S., Fallon, J.K., Michell, A.R., Broge, T., Suscovich, T.J., Streeck, H., and Alter, G. (2019). A high-throughput, bead-based, antigen-specific assay to assess the ability of antibodies to induce complement activation. J. Immunol. Methods *473*, 112630.

Goenka, A., Halliday, A., Gregorova, M., Milodowski, E., Thomas, A., Williamson, M.K., Baum, H., Oliver, E., Long, A.E., Knezevic, L., et al. (2021). Young infants exhibit robust functional antibody responses and restrained IFN-γ production to SARS-CoV-2. Cell Rep. Med. *2*, 100327.

Grazioli, S., Tavaglione, F., Torriani, G., Wagner, N., Rohr, M., L'Huillier, A.G., Leclercq, C., Perrin, A., Bordessoule, A., Beghetti, M., et al. (2021). Immunological assessment of pediatric multisystem inflammatory syndrome related to COVID-19. J. Pediatric Infect. Dis. Soc. *10*, 706–713.

Heald-Sargent, T., Muller, W.J., Zheng, X., Rippe, J., Patel, A.B., and Kociolek, L.K. (2020). Age-related differences in nasopharyngeal severe acute respiratory syndrome coronavirus 2 (SARS-CoV-2) levels in patients with mild to moderate coronavirus disease 2019 (COVID-19). JAMA Pediatr. *174*, 902–903.

Heinonen, S., Velazquez, V.M., Ye, F., Mertz, S., Acero-Bedoya, S., Smith, B., Bunsow, E., Garcia-Mauriño, C., Oliva, S., Cohen, D.M., et al. (2020). Immune profiles provide insights into respiratory syncytial virus disease severity in young children. Sci. Transl. Med. *12*, eaaw0268.

Henry, B.M., Lippi, G., and Plebani, M. (2020). Laboratory abnormalities in children with novel coronavirus disease 2019. Clin. Chem. Lab. Med. *58*, 1135–1138.

Iwasaki, A., and Yang, Y. (2020). The potential danger of suboptimal antibody responses in COVID-19. Nat. Rev. Immunol. *20*, 339–341.

Jaume, M., Yip, M.S., Cheung, C.Y., Leung, H.L., Li, P.H., Kien, F., Dutry, I., Callendret, B., Escriou, N., Altmeyer, R., et al. (2011). Anti-severe acute respiratory syndrome coronavirus spike antibodies trigger infection of human immune cells via a pH- and cysteine protease-independent FcγR pathway. J. Virol. *85*, 10582–10597.

Koopmans, M., de Bruin, E., Godeke, G.J., Friesema, I., van Gageldonk, R., Schipper, M., Meijer, A., van Binnendijk, R., Rimmelzwaan, G.F., de Jong, M.D., et al. (2012). Profiling of humoral immune responses to influenza viruses by using protein microarray. Clin. Microbiol. Infect. *18*, 797–807.

Li, S., Rouphael, N., Duraisingham, S., Romero-Steiner, S., Presnell, S., Davis, C., Schmidt, D.S., Johnson, S.E., Milton, A., Rajam, G., et al. (2014). Molecular signatures of antibody responses derived from a systems biology study of five human vaccines. Nat. Immunol. *15*, 195–204.

Liao, Y., Smyth, G.K., and Shi, W. (2014). featureCounts: an efficient general purpose program for assigning sequence reads to genomic features. Bioinformatics *30*, 923–930.

Lu, X., Zhang, L., Du, H., Zhang, J., Li, Y.Y., Qu, J., Zhang, W., Wang, Y., Bao, S., Li, Y., et al.; Chinese Pediatric Novel Coronavirus Study Team (2020). SARS-CoV-2 infection in children. N. Engl. J. Med. *382*, 1663–1665.

Lucas, C., Wong, P., Klein, J., Castro, T.B.R., Silva, J., Sundaram, M., Ellingson, M.K., Mao, T., Oh, J.E., Israelow, B., et al.; Yale IMPACT Team (2020). Longitudinal analyses reveal immunological misfiring in severe COVID-19. Nature *584*, 463–469.

Matias, G., Taylor, R.J., Haguinet, F., Schuck-Paim, C., Lustig, R.L., and Fleming, D.M. (2016). Modelling estimates of age-specific influenza-related hospitalisation and mortality in the United Kingdom. BMC Public Health *16*, 481.

Meyer, B., Reimerink, J., Torriani, G., Brouwer, F., Godeke, G.J., Yerly, S., Hoogerwerf, M., Vuilleumier, N., Kaiser, L., Eckerle, I., and Reusken, C. (2020). Validation and clinical evaluation of a SARS-CoV-2 surrogate virus neutralisation test (sVNT). Emerg. Microbes Infect. *9*, 2394–2403.

Midulla, F., Cristiani, L., and Mancino, E. (2020). Will children reveal their secret? The coronavirus dilemma. Eur. Respir. J. *55*, 2001617.

Moratto, D., Giacomelli, M., Chiarini, M., Savarè, L., Saccani, B., Motta, M., Timpano, S., Poli, P., Paghera, S., Imberti, L., et al. (2020). Immune response in children with COVID-19 is characterized by lower levels of T-cell activation than infected adults. Eur. J. Immunol. *50*, 1412–1414.

Mudd, P.A., Crawford, J.C., Turner, J.S., Souquette, A., Reynolds, D., Bender, D., Bosanquet, J.P., Anand, N.J., Striker, D.A., Martin, R.S., et al. (2020). Distinct inflammatory profiles distinguish COVID-19 from influenza with limited contributions from cytokine storm. Sci. Adv. *6*, eabe3024.

Munro, A.P.S., and Faust, S.N. (2020). COVID-19 in children: current evidence and key questions. Curr. Opin. Infect. Dis. *33*, 540–547.

Muus, C., Luecken, M.D., Eraslan, G., Sikkema, L., Waghray, A., Heimberg, G., Kobayashi, Y., Vaishnav, E.D., Subramanian, A., Smillie, C., et al.; NHLBI LungMap Consortium; Human Cell Atlas Lung Biological Network (2021). Single-cell meta-analysis of SARS-CoV-2 entry genes across tissues and demographics. Nat. Med. *27*, 546–559.

Neeland, M.R., Bannister, S., Clifford, V., Dohle, K., Mulholland, K., Sutton, P., Curtis, N., Steer, A.C., Burgner, D.P., Crawford, N.W., et al. (2021). Innate cell profiles during the acute and convalescent phase of SARS-CoV-2 infection in children. Nat. Commun. *12*, 1084.

Ng, K.W., Faulkner, N., Cornish, G.H., Rosa, A., Harvey, R., Hussain, S., Ulferts, R., Earl, C., Wrobel, A.G., Benton, D.J., et al. (2020). Preexisting and de novo humoral immunity to SARS-CoV-2 in humans. Science *370*, 1339–1343.

Perlman, S., and Dandekar, A.A. (2005). Immunopathogenesis of coronavirus infections: implications for SARS. Nat. Rev. Immunol. *5*, 917–927.

Pierce, C.A., Preston-Hurlburt, P., Dai, Y., Aschner, C.B., Cheshenko, N., Galen, B., Garforth, S.J., Herrera, N.G., Jangra, R.K., Morano, N.C., et al. (2020). Immune responses to SARS-CoV-2 infection in hospitalized pediatric and adult patients. Sci. Transl. Med. *12*, 12.

Pierce, C.A., Sy, S., Galen, B., Goldstein, D.Y., Orner, E., Keller, M.J., Herold, K.C., and Herold, B.C. (2021). Natural mucosal barriers and COVID-19 in children. JCI Insight *6*, eabd5487.

R Core Team. (2018). R: A Language and Environment for Statistical Computing (R Foundation for Statistical Computing). https://www.R-project.org.

Reusken, C., Mou, H., Godeke, G.J., van der Hoek, L., Meyer, B., Müller, M.A., Haagmans, B., de Sousa, R., Schuurman, N., Dittmer, U., et al. (2013). Specific serology for emerging human coronaviruses by protein microarray. Euro Surveill. *18*, 20441.

Riphagen, S., Gomez, X., Gonzalez-Martinez, C., Wilkinson, N., and Theocharis, P. (2020). Hyperinflammatory shock in children during COVID-19 pandemic. Lancet *395*, 1607–1608.

Robinson, M.D., McCarthy, D.J., and Smyth, G.K. (2010). edgeR: a Bioconductor package for differential expression analysis of digital gene expression data. Bioinformatics *26*, 139–140.

Saheb Sharif-Askari, N., Saheb Sharif-Askari, F., Alabed, M., Temsah, M.H., Al Heialy, S., Hamid, Q., and Halwani, R. (2020). Airways expression of SARS-CoV-2 receptor, ACE2, and TMPRSS2 is lower in children than adults and increases with smoking and COPD. Mol. Ther. Methods Clin. Dev. *18*, 1–6.

Schouten, L.R., van Kaam, A.H., Kohse, F., Veltkamp, F., Bos, L.D., de Beer, F.M., van Hooijdonk, R.T., Horn, J., Straat, M., Witteveen, E., et al.; MARS consortium (2019). Age-dependent differences in pulmonary host responses in ARDS: a prospective observational cohort study. Ann. Intensive Care *9*, 55.

Schuler, B.A., Habermann, A.C., Plosa, E.J., Taylor, C.J., Jetter, C., Negretti, N.M., Kapp, M.E., Benjamin, J.T., Gulleman, P., Nichols, D.S., et al.; Vanderbilt COVID-19 Consortium Cohort; Human Cell Atlas Biological Network (2020). Age-determined expression of priming protease TMPRSS2 and localization of SARS-CoV-2 in lung epithelium. J. Clin. Invest. *131*, e140766.

Selva, K.J., van de Sandt, C.E., Lemke, M.M., Lee, C.Y., Shoffner, S.K., Chua, B.Y., Davis, S.K., Nguyen, T.H.O., Rowntree, L.C., Hensen, L., et al. (2021). Systems serology detects functionally distinct coronavirus antibody features in children and elderly. Nat. Commun. *12*, 2037.

Shi, T., McAllister, D.A., O'Brien, K.L., Simoes, E.A.F., Madhi, S.A., Gessner, B.D., Polack, F.P., Balsells, E., Acacio, S., Aguayo, C., et al.; RSV Global Epidemiology Network (2017). Global, regional, and national disease burden estimates of acute lower respiratory infections due to respiratory syncytial virus in young children in 2015: a systematic review and modelling study. Lancet *390*, 946–958.

Stringhini, S., Wisniak, A., Piumatti, G., Azman, A.S., Lauer, S.A., Baysson, H., De Ridder, D., Petrovic, D., Schrempft, S., Marcus, K., et al. (2020). Seroprevalence of anti-SARS-CoV-2 IgG antibodies in Geneva, Switzerland (SERO-CoV-POP): a population-based study. Lancet *396*, 313–319.

Upham, J.W., Zhang, G., Rate, A., Yerkovich, S.T., Kusel, M., Sly, P.D., and Holt, P.G. (2009). Plasmacytoid dendritic cells during infancy are inversely associated with childhood respiratory tract infections and wheezing. J. Allergy Clin. Immunol. *124*, 707, 13.e2.

Vakkila, J., Thomson, A.W., Vettenranta, K., Sariola, H., and Saarinen-Pihkala, U.M. (2004). Dendritic cell subsets in childhood and in children with cancer: relation to age and disease prognosis. Clin. Exp. Immunol. *135*, 455–461.

Valiathan, R., Ashman, M., and Asthana, D. (2016). Effects of ageing on the immune system: infants to elderly. Scand. J. Immunol. *83*, 255–266.

van Tol, S., Mögling, R., Li, W., Godeke, G.J., Swart, A., Bergmans, B., Brandenburg, A., Kremer, K., Murk, J.L., van Beek, J., et al. (2020). Accurate serology for SARS-CoV-2 and common human coronaviruses using a multiplex approach. Emerg. Microbes Infect. *9*, 1965–1973.

Verdoni, L., Mazza, A., Gervasoni, A., Martelli, L., Ruggeri, M., Ciuffreda, M., Bonanomi, E., and D'Antiga, L. (2020). An outbreak of severe Kawasaki-like disease at the Italian epicentre of the SARS-CoV-2 epidemic: an observational cohort study. Lancet *395*, 1771–1778.

Viner, R.M., Mytton, O.T., Bonell, C., Melendez-Torres, G.J., Ward, J., Hudson, L., Waddington, C., Thomas, J., Russell, S., van der Klis, F., et al. (2021). Susceptibility to SARS-CoV-2 infection among children and adolescents compared with adults: a systematic review and meta-analysis. JAMA Pediatr. *175*, 143–156.

Wei, L.L., Wang, W.J., Chen, D.X., and Xu, B. (2020). Dysregulation of the immune response affects the outcome of critical COVID-19 patients. J. Med. Virol. *92*, 2768–2776.

Weisberg, S.P., Connors, T.J., Zhu, Y., Baldwin, M.R., Lin, W.H., Wontakal, S., Szabo, P.A., Wells, S.B., Dogra, P., Gray, J., et al. (2021). Distinct antibody responses to SARS-CoV-2 in children and adults across the COVID-19 clinical spectrum. Nat. Immunol *22*, 25–31.

Wong, L.S.Y., Loo, E.X.L., Kang, A.Y.H., Lau, H.X., Tambyah, P.A., and Tham, E.H. (2020). Age-related differences in immunological responses to SARS-CoV-2. J. Allergy Clin. Immunol. Pract. *8*, 3251–3258.

Wu, H., Zhu, H., Yuan, C., Yao, C., Luo, W., Shen, X., Wang, J., Shao, J., and Xiang, Y. (2020). Clinical and immune features of hospitalized pediatric patients with coronavirus disease 2019 (COVID-19) in Wuhan, China. JAMA Netw. Open *3*, e2010895.

Yip, M.S., Leung, N.H., Cheung, C.Y., Li, P.H., Lee, H.H., Daëron, M., Peiris, J.S., Bruzzone, R., and Jaume, M. (2014). Antibody-dependent infection of human macrophages by severe acute respiratory syndrome coronavirus. Virol. J. *11*, 82.

Yonker, L.M., Neilan, A.M., Bartsch, Y., Patel, A.B., Regan, J., Arya, P., Gootkind, E., Park, G., Hardcastle, M., St John, A., et al. (2020). Pediatric severe acute respiratory syndrome coronavirus 2 (SARS-CoV-2): clinical presentation, infectivity, and immune responses. J. Pediatr. *227*, 45–52.e5.

Zhang, Q., Bastard, P., Liu, Z., Le Pen, J., Moncada-Velez, M., Chen, J., Ogishi, M., Sabli, I.K.D., Hodeib, S., Korol, C., et al.; COVID-STORM Clinicians; COVID Clinicians; Imagine COVID Group; French COVID Cohort Study Group; CoV-Contact Cohort; Amsterdam UMC Covid-19 Biobank; COVID Human Genetic Effort; NIAID-USUHS/TAGC COVID Immunity Group (2020). Inborn errors of type I IFN immunity in patients with life-threatening COVID-19. Science *370*, eabd4570.

Zheng, J., Wang, Y., Li, K., Meyerholz, D.K., Allamargot, C., and Perlman, S. (2021). Severe acute respiratory syndrome coronavirus 2-induced immune activation and death of monocyte-derived human macrophages and dendritic cells. J. Infect. Dis. *223*, 785–795.

Zimmermann, P., and Curtis, N. (2020). Coronavirus Infections in Children Including COVID-19: An Overview of the Epidemiology, Clinical Features, Diagnosis, Treatment and Prevention Options in Children. Pediatr. Infect. Dis. J. *39*, 355–368.

STAR★METHODS

KEY RESOURCES TABLE

REAGENT or RESOURCE	SOURCE	IDENTIFIER
Antibodies		
anti-human CD3- BV786	BD Biosciences	Cat# 565491
anti-human CD20- BUV737	BD Biosciences	Cat# 612848
anti-human CD56-PECF594	BD Biosciences	Cat# 562289
anti-human HLA-DR-PerCp 5.5	BD Biosciences	Cat# 560652
anti-human CD123-PE-Cy7	eBioscience	Cat# 25-1239-42
anti-human CD11c-AF700	BD Biosciences	Cat# 561352
anti-human CD14-PB	BD Biosciences	Cat# 558121
anti-human CD16-FITC	BD Biosciences	Cat# 561308
anti-human CD86-PE	BD Biosciences	Cat# 555658
anti-human CD40-APC-H7	BD Biosciences	Cat# 561211
anti-human CD1c-APC	Miltenyi	Cat# 130-113-299
anti-human CD15-BV650	BD Biosciences	Cat# 564232
anti-human CD141 BV711	BD Biosciences	Cat# 563155
PE anti-human IgG	Biolegend	Cat# 409304
PE anti-Human IgG1	Southern Biotech	Cat#9052-09
PE anti-Human IgG3	Southern Biotech	Cat#9210-09
Biotin anti-human C3d	Quidel	Cat#A207
Biotin anti-human IgG	Jackson	Cat# 709-066-098
Chemicals, peptides, and recombinant proteins		
RBD protein from SARS-CoV-2	Sino Biological	Cat#40592-VNAH
Trimerized Spike protein from SARS-CoV-2	N/A	kindly provided by the protein production core facility of the EPFL, Lausanne, CH)
Nucleocapsid protein from SARSCoV-2	ProSpec	Cat#sars-040
NHS (N-hydroxysuccinimide)	Thermo Scientific	Cat#24520
Spike protein S1 subunit	Sino biological	Cat#40591-V08H
EDC(1-ethyl-3-(3-dimethylaminopropyl) carbodiimide hydrochloride)	Thermo Scientific	Cat#77149
Melon Gel Resin	Thermo Scientific	Cat#45208
human complement serum	Sigma	Cat#S1764
Streptavidin-RPE	Prozyme/Agilent	Cat#PJ31S-1
EZ-Link NHS-LC-Biotin	Thermo Scientific	Cat#21343
Zeba Spin Desalting Columns	Thermo Scientific	Cat#89883
FluoSpheres NeutrAvidin beads	Thermo Scientific	Cat#F8776
BD,CellFIX	BD Biosciences	Cat# 340181
FACS Lysing Solution	BD Biosciences	Cat# 349202
CountBright absolute counting beads	Thermofisher	Cat# #C36950
Recombinant human IL-2	Peprotech	Cat# 200-02
R848	Chemdea	Cat# CD0271
Streptavidin-POD conjugate	Roche	Cat# #11089153001
Critical commercial assays		
SARS-CoV-2 Neutralization Antibody Detection Kit	Genscript	Cat#L00847
Luminex Performance Human Fixed Immunotherapy Magnetic Panel (24-Plex)	R&D Systems	Cat#LKTM010

(*Continued on next page*)

Continued

REAGENT or RESOURCE	SOURCE	IDENTIFIER
VersaComp Antibody Capture Bead Kits	Beckam Coulter	Cat#B22804
Stranded Total RNA Ribo-Zero Plus kit	Illumina	Cat#20040529
Experimental models: Cell lines		
THP-1	ATCC®	TIB-202
Deposited data		
Raw and analyzed RNaseq data	This paper	GEO: GSE166190
Software and algorithms		
FacsDiva	BD Biosciences	https://www.bdbiosciences.com/en-us.
FlowJo	FlowJo	https://www.flowjo.com/solutions/flowjo/downloads
Prism	GraphPad	https://www.graphpad.com/scientific-software/prism/
featureCounts	Bioconductor	Liao et al., 2014
edgeR	Bioconductor	Robinson et al., 2010
R	R Foundation	https://www.r-project.org/
STAR	GitHub	https://github.com/alexdobin/STAR/releases

RESOURCE AVAILABILITY

Lead contact

Further information and requests for resources and reagents should be directed to and will be fulfilled by the lead contact, Arnaud Didierlaurent (arnaud.didierlaurent@unige.ch)

Materials availability

This study did not generate new unique reagents.

Data and code availability

The RNA-seq data have been deposited to the Gene Expression Omnibus (GEO) under accession number GEO: GSE166190.

This paper does not report original code.

Any additional information required to reanalyze the data reported in this paper is available from the lead contact upon request.

EXPERIMENTAL MODEL AND SUBJECT DETAILS

Setting, study population, and design

This prospective observational study was conducted at the Geneva University Hospitals (HUG), Switzerland from March 2020 to January 2021 covering 2 epidemic waves and was approved by the Geneva Cantonal Ethics Commission (2020-00516). Informed consent was obtained from all adult participants, and from the legally appointed representatives (parents) of all child participants. 'Case patients' were eligible for inclusion if they had laboratory-confirmed SARS-CoV-2 infection with diagnosis in the two preceding days and 'contacts' were eligible if they were household contacts of the enrolled patient. An enrolled patient was followed for 8 weeks as the index case; his or her household contacts were followed for two weeks. If a contact became SARS-CoV-2–positive at any point and granted informed consent, he or she became a case patient and was followed for another six weeks. Further details on study design and flow are shown in Figure S1. Age and gender of COVID-19 patients and negative contacts recruited in this study are reported in Table S1. The analysis presented here was performed on study participants selected as follows. All SARS-CoV-2–positive children recruited in a total of 10 clusters were selected together with the infected adults present in these clusters (''matched adults''). Nine additional adults showing a similar symptom profile these ''matched adults'' were also included from other clusters. We then excluded those with SARS-CoV-2+ antibodies at first visit to avoid the possibility that infection could have occurred sometime before symptoms onset and diagnosis. Among 31 contacts who remained negative in the study, we selected all children (n = 4) and 5 adults from the same cluster as controls. Complete blood counts were performed in the HUG routine clinical laboratory.

METHODS DETAILS

SARS-CoV-2 RNA quantification

Quantitative real time (RT)-PCR was performed on all nasopharyngeal swabs. All initial samples were tested as part of the diagnostic SARS-CoV-2 routine testing on the Cobas 6800 (Roche) and viral loads calculated as described previously (Baggio et al., 2020). All follow-up specimens were tested and quantified with the Charité RT-PCR protocol (Corman et al., 2020) using *in vitro*-transcribed RNA for quantification (European Virus Archive—Global project; https://www.european-virus-archive.com/) after RNA extraction with the NucliSens eMAG extraction kit (BioMérieux, France). All viral loads are reported as SARS-CoV-2 genome copies/ml of original sample collected in viral transport medium. Nasopharyngeal swabs were screened by acid nucleic detection for the presence of influenza A and B virus, respiratory syncytial virus (RSV) A and B, parainfluenza 1 to 4, human metapneumovirus, rhinoviruses, enteroviruses, bocavirus 1, adenovirus and human coronaviruses 229E, OC43, HKU1 and NL63 using either an in-house RT-PCR panel or the multiplex RT-PCR Fast-Track Diagnostics Resp21 commercial panel (Fast-Track Diagnostics, Esch-sur-Alzette, Luxembourg).

RNA-sequencing of whole blood

Blood samples were collected directly in PAXgene® Blood RNA Tube (BD Biosciences) at different times post-infection or enrollment and stored within 4-6 hours of collection at −80°C until extraction. RNA extraction was performed via the PAXgene Blood miRNA Kit on the QIAcube instrument (QIAGEN) following the manufacturer's protocol. RNA concentration and quality were assessed by using the Qubit instrument (Invitrogen) and the Agilent 2100 Bioanalyzer, respectively. The Stranded Total RNA Ribo-Zero Plus kit from Illumina was used for the library preparation with 100 ng of total RNA as input. Library molarity and quality were assessed with the Qubit and Tapestation using a DNA High sensitivity chip (Agilent Technologies). Libraries were pooled at 2 nM for clustering and sequenced on an Illumina HiSeq 4000 sequencer for a minimum of 30 million single-end 100 reads per sample.

RNA-sequencing data analysis

Reads were mapped to the genome (GRCh38.96) using STAR (2.4.0j) (Dobin et al., 2013) keeping only uniquely mapped reads. Reads overlapping annotated genes of GRCh38.96 were reported using featureCounts (version 1.4.6-p1) (Liao et al., 2014). Gene expressions were reported as normalized in RPKM. Blood Transcription Modules (BTMs) were downloaded from https://github.com/shuzhao-li/BTM (Li et al., 2014). In a first round of analysis, we calculated average log2 fold changes to the mean expression values of all genes involved in each BTM per each temporal interval, defined according to DPOS, and per age group. BTMs with average value above log2(1.5) in at least one interval in one age group were considered as enriched and reported in violin plots representing the log2 fold changes to the mean expression levels. Color intensity represents the average value. Heatmaps report genes belonging to the enriched BTMs.

For all differential expression analysis, gene expressions were reported as raw counts and normalized in RPKM in order to filter out genes with low expression value (1 RPKM) before calling for differentially expressed genes (DEGs). Library size normalizations and differential gene expression calculations were performed using the package edgeR (Robinson et al., 2010) designed for the R software (R Core Team [2018]). Only genes having a significant fold-change (Benjamini-Hochberg corrected $p < 0.05$) were considered for the rest of the RNA-seq analysis. Paired and unpaired comparisons were performed.

For each group of paired or unpaired comparisons, (e.g., interval 1/2/3/4 versus interval 5 or children versus adults at interval 1 or 2) BTMs were selected by the Fisher test (Odds ratio < 2 and $p < 0.05$). Contingency tables considering the differentially expressed genes (DEGs; $p < 0.05$ and abs(log2FC) > 1) and the genes included in each BTM were constructed. After BTMs selection, the averaged log2FC of the DEGs belonging to each BTM, as well as the percentage of BTM genes being differentially expressed were reported on graphs. The RNA-seq data have been deposited to the Gene Expression Omnibus (GEO) under accession number GEO: GSE166190.

Cytokine measurement in plasma

Cytokine concentrations in cryopreserved plasma from patients or healthy controls were measured by magnetic Luminex assay (R&D Systems), according to the supplier's instructions. Data were acquired on a Bio-Plex 200 array reader (Bio-Rad Laboratories). Five-parameter logistic regression curve (Bio-Plex Manager 6.0) was used to calculate sample concentrations. We used a 23-plex panel and measured the levels of CD40L, GM-CSF, Granzyme B, IFN-α, IFN-γ, IL1-α, IL1-β, IL1R-α, IL-2, IL-4, IL-6, IL-8, IL-10, IL-12p70, IL-13, IL17A, IL-33, CXCL10, CCL2, CCL3, CCL4, PD-L1, TNF-α. Results below the lower limit of detection were assigned a value corresponding to 50% of the value of the lowest standard dilution. We only report cytokines with significant temporal changes, detected by using a mixed-effect model with measures nested in individuals and an interaction between groups and intervals, with a Bonferroni-Holm correction. We used R 4.0.3, packages nlme (version 3.1-149) for mixed-effect models and phia (version 0.2-1) for post-hoc interaction analyses. Outcomes were transformed using a log10-transformation.

Blood cell phenotyping by flow cytometry

Whole blood collected in BD Vacutainer® blood collection tubes (BD, #368886) was processed within 4h of procurement. The whole blood was resuspended in 1x FACS Lysing Solution (BD, #349202), incubated for 9 minutes and centrifugated at room temperature (RT), 1500 rpm, for 5 minutes. After partial removal of the supernatant, the pellet was resuspended in the remaining 3 mL and

transferred in cryotubes that were immediately frozen in liquid nitrogen until flow cytometry analysis. The day of the flow cytometry staining, cells were thawed, spun, and transferred into a 96-well round plate. After two washes with PBS plus 0.5% BSA, cells were stained for 30 min at RT with a 13-color panel: CD3-BV786, CD20-BUV737, CD56-PECF594, HLA-DR-PerCp 5.5, CD123-PE-Cy7, CD11c-AF700, CD14-PB, CD16-FITC, CD86-PE, CD40-APC-H7, CD1c-APC, CD15-BV650, CD141-BV711. After two washes with PBS, cells were resuspended in PBS and CountBright absolute counting beads (Thermofisher, #C36950) were added. The cells were analyzed using a BD LSRFortessa. Cytometer setup, tracking beads (BD Biosciences), and rainbow calibration particles (8 peaks; Sphero; BD Biosciences) were used to calibrate the machine prior to each run to ensure that machine performance remained the same. Compensation beads (VersaComp Antibody Capture Bead Kits; Beckam Coulter) were used as single-stain positive and negative controls. Compensated samples were analyzed in FlowJo (TreeStar). Cell numbers were calculated by using counting beads and normalized to the initial volume of blood processed per sample.

Analysis of antibody response

SARS-CoV-2 RBD (SinoBiological #40592-VNAH), SARS-CoV-2 complete trimerized spike protein (S) (kindly provided by the protein production core facility of the EPFL, Lausanne, CH), and SARS-CoV-2 nucleocapsid (N) protein (ProSpec #sars-040) were used to profile the SARS-CoV-2-specific humoral immune response. Titers of antigen-specific antibody isotypes and subclasses were assessed using a 96-well based customized multiplexed Luminex assay. Briefly, antigens were coupled by covalent NHS-ester linkages via EDC and NHS (Pierce #77149 and #24520, respectively) to fluorescent carboxyl modified microspheres (Luminex). Antigen-coupled microspheres were then washed using magnetic separation and incubated 2 hours at RT with plasma samples at appropriate dilution: 1:200 for IgG, IgG1 and IgG3, titration. Antigen-specific antibody titers were detected using 0.65 μg/ml of PE-coupled detection antibody for each isotype and subclass, including IgG (Biolegend #409304), IgG1 (Southern Biotech #9052-09), and IgG3 (Southern Biotech #9210-09). Antigen-antibody reactions were read on BioPlex-200 equipment (Bio-Rad) and the results were expressed as median fluorescence intensity. Serum from negative children and adults that have been collected before COVID-19 pandemic were used as additional controls.

Antibody-dependent complement deposition (ADCD) was quantified using a 96-well based customized multiplexed luminex assay, as described previously (Fischinger et al., 2019). Bulk IgG was purified from other serum proteins using Melon Gel Resin (Thermo Scientific #45208) according to the manufacturer's instructions. Purified IgG at 1:10 dilution, was incubated with SARS-CoV-2 RBD- or S-coupled beads (1000 beads/well/antigen) for 2 h at 37°C. Unbound antibodies were removed by washing with 1% BSA in PBS. After washing, each sample was incubated with human complement serum (Sigma #S1764) at a concentration of 1:50 at 37°C for 30 min. Samples were washed, sonicated, and incubated at RT for 30 min with biotinylated monoclonal anti-human C3d (1 μg/ml, Quidel #207). After washing, Streptavidin-RPE (1 μg/ml; Prozyme #PJ31S) was added to each well and incubated at 37°C in the dark for 1h. After a final wash and sonication, samples were resuspended in 100μl of 1% BSA in PBS and complement deposition was determined on a BioPlex-200 equipment (Bio-Rad) and measured as median fluorescence intensity. Assays performed without IgG and with heat-inactivated human complement serum were used as negative controls.

Antibody-dependent cellular phagocytosis (ADCP) was assessed using the human monocyte cell line THP-1 (ATCC #TIB-202), as previously described (Ackerman et al., 2011). Prior the assay, 0.3 mg/ml of the S antigen were biotinylated using EZ-Link NHS-LC-LC-Biotin (Thermo #21343) for 30 min at 37°C (1 mole of antigen for 50 moles of biotin). The biotinylated S was then purified using zeba spin desalting columns (Thermo #89883) and then coupled to FluoSpheres NeutrAvidin beads (Thermo #F8776) for 2 h at 37°C. Antigen-conjugated beads were then washed twice with 0.1% BSA in PBS and diluted 100-fold in this buffer. In a 96-well clear microplate (Greiner #650180), 10 μl of antigen-conjugated beads were incubated for 2h at 37°C with 10 μl of diluted purified IgG (1:50). After incubation, wells were washed twice with PBS and centrifugated (2000 g, 10 minutes). 200 μl of $0.5x10^5$ THP-1 cell/ml were added to each well and incubated 16 hours at 37°C, 5% C02. Finally, cells were centrifuged (125 g, 10 min) and 100 μl of the supernatant was substituted by 100 μl of 1X CellFIX (BD #340181). The acquisition was done by using a LSR-Fortessa (BD). Results were expressed as phagocytic score: $FITC^{+}_{frequency}$ X $FITC^{+}_{mean}$*10^{-4}. Assays performed without IgG and with a pool of IgG obtained from healthy blood donors before the COVID-19 pandemic were used as negative controls.

Neutralization assay (sVNT)

Neutralization capacity of serum samples was assessed using a commercially available surrogate neutralizations assay (sVNT, cPass SARS-CoV-2 Neutralization Antibody Detection Kit, # L00847, Genscript). A recombinant RBD-HRP fusion protein was mixed with serum samples (or positive and negative control sera) at a dilution of 1:10 and incubated for 30min at 37°C. Controls were measured in duplicate and samples in singular after experimental validation of inter-assay variability where the coefficient of variation was found to range between 0.2%–2.8% for high-titer samples and 10%–20% for samples around the cut-off (Meyer et al., 2020). This mixture was transferred to ELISA plates coated with recombinant ACE2 protein and incubated for 15min at 37°C. Supernatant was removed, the plate washed 4x with the washing buffer and 100μl of tetramethylbenzidine substrate was added for 15 minutes. The reaction was stopped by adding 50μl of stop solution. The plates were read at 450nm and % reduction was calculated using the negative control as a reference. On each plate we included a 2-fold dilution series of a reference serum pool (pre-diluted in PBS + 1% BSA). The value of the neat reference serum pool was arbitrarily set to 100 AU/ml. We observed a linear range of the sVNT from 0% up to 80% reduction. AU/ml values for all samples were interpolated by using the standard curve of the same plate. The final cut-off (1.43 AU/ml) was defined as the mean AU/ml + 3x standard deviation of 20 negative samples.

IgG antibodies to human coronaviruses (HCoVs) determined by protein microarray

HCoV-PMA slides were essentially produced as previously described (Koopmans et al., 2012). Antigens (HCoV-OC43, HCoV-HKU1, HCoV-229E and HCoV-NL63 S1 at 0.75 mg/ml; SARS-CoV-2 S1 at 0.65 mg/ml) were spotted in duplicate in three drops of 333 pL each on 24-pads nitrocellulose-coated slides (ONCYTE AVID, GraceBio Labs,Bend, USA) by using a non-contact Marathon Arrayjet micro-array spotter (Roslin, UK). Printed microarray slides were used for detection of IgG antibodies as previously described (Reusken et al., 2013; van Tol et al., 2020).

Memory B cell analysis by enzyme-linked immunospot (ELISpot) assay

S1-specific MBCs were quantified by ELISpot assay using 96-well multiscreen-HA filter nitrocellulose plates (Millipore) coated with S1 protein (100 ng/well, Sino biological, #40591-V08H) and anti-human IgG (1 μg/well, Jackson, Ref 709-005-149). The ELISPOT plates were incubated overnight at 4°C, washed twice in PBS, and blocked with RPMI (GIBCO) plus 10% (v/v) Fetal Bovine Serum (FBS; Bioconcept). Cryopreserved PBMCs were thawed and plated at an initial number of $1x10^6$ /well and stimulated with a combination of R848 (1μg/ml, Chemdea #CD0271)) and IL-2 (10 ng/ml, Peprotech #200-02) in RPMI supplemented (FBS 10%, 1% Penicillin, Streptomycin, L-Glutamine and betamercaptoetanol) at 37°C, 5% CO2 for 6 days, and then cells were washed with RPMI supplemented and plated in the ELISPOT plates in a 3-fold dilution. After six hours of incubation (37°C and 5% CO2), we added a biotinylated anti-human IgG (Jackson ImmunoResearch, #709-066-098) followed by horseradish peroxidase (HRP)-conjugated streptavidin (streptavidin-POD conjugate, Roche, #11089153001) to detect antibody secreting memory B cells. Plates were first washed with PBS-T and then with PBS. Detection was performed by adding 100 ul of 3-amino-9-ethylcarbazole substrate buffer for 30 min in the dark until spots appeared. The reaction was stopped by thorough washing with cold tap water. Plates were air-dried, scanned (ELISPOT Reader CTL) and spots were manually counted.

QUANTIFICATION AND STATISTICAL ANALYSIS

Non-transcriptomic data were further analyzed using Prism 9.0 (GraphPad Software) and presented as specified in figure legends. Differences between groups were analyzed as described in figure legends. $p < 0.05$ was considered statistically significant.